M.Tech Dissertation Report

Analysis and Characterization of Geometric Objects on Tetrahedral Grid

Girish Koshti
Enrollment No.: 16535011

Supervisor: Dr. Ranita Biswas
Computer Science and Engineering Department
Indian Institute of Technology, Roorkee

May 18, 2018

Declaration

I certify that

a. The work contained in the dissertation is original and has been done by myself under the general supervision of my supervisor.

b. The work has not been submitted to any other Institute for any degree or diploma.

c. I have followed the guidelines provided by the Institute in writing the dissertation.

d. I have conformed to the norms and guidelines given in the Ethical Code of Conduct of the Institute.

e. Whenever I have used materials (data, theoretical analysis, and text) from other sources, I have given due credit to them by citing them in the text of the dissertation and giving their details in the references.

f. Whenever I have quoted written materials from other sources, I have put them under quotation marks and given due credit to the sources by citing them and giving required details in the references.

Girish Koshti

Roll No.: 16535011

Certificate

This is to certify that the dissertation entitled *Analysis and Characterization of Geometric Objects on Tetrahedral Grid* by **Girish Koshti** to Indian Institute of Technology, Roorkee, is a record of bonafide research work carried under my supervision and is worthy of consideration for the award of the degree of Master of Technology of the Institute.

Dr. Ranita Biswas

Assistant Professor

Department of Computer Science and Engineering

Indian Institute of Technology Roorkee, India

Abstract

A *grid* usually is two or more sets of parallel lines in 2D or planes in 3D that intersect one another (called as grid points) at particular angle. It divides the plane or space into many congruent *polytopes*. Most common grids are square (in 2D) and cubical (in 3D). Grid is used in digital modeling of geometric objects. A digital model can be represented by a set of 2D pixels or 3D voxels. The choice of shape of pixel or of voxel is very important in digital modeling. *Circular pixels* and *spherical voxels* have this interesting property that all points on their surface is equidistant from grid point which is not the case in square pixels or cubical voxels. Spherical voxels are not stable on cubical grid. Stable self-alignment of spheres in 3D forms a tetrahedron. A *simplex* is the generalization of tetrahedron and triangle to *n* dimensions. 2-simplex grid is equivalent to triangular and 3-simplex grid is equivalent to tetrahedral grid. The dual of triangular grid is hexagonal grid. The notion of simplex grid topologically simplifies study of polytopes. Our aim is to analyze simplex grid and characterize basic geometric shapes on it.

Keywords: simplex grid, triangle, tetrahedron, circular pixel, spherical voxel.

Contents

List of Figures

List of Tables

1 Introduction

With the advancement of 3D computer graphics we see a noticeable progress towards digital modeling of geometric objects. Digital Representation of geometric objects requires characterization and discretization of geometric elements namely lines, circles and arcs. Geometric objects are digitally represented on a grid. A *grid* usually is two or more sets of parallel lines in 2D or planes in 3D that intersect one another at particular angle. These intersection points are called as grid points. It divides the plane or space into many congruent *polytopes*. Most common polytopes on grids are *square* (in 2D) and *cube* (in 3D). A grid can be represented by $\mathbb{Z}^2$ in 2D or $\mathbb{Z}^3$ in 3D when we deal with this square or cubic grid. There are two type of *grid models* to a represent grid, namely grid point model and grid cell model as defined in [9].

For the sake of simplicity we are explaining the notion of these models with respect to square (and cubic in 3D) grids only. The basic concept is replicated to other grid shapes. In the *Grid point* model, a 2D grid $\mathbb{G}$ is infinite grid $\mathbb{Z}^2$ or $m \times n$ sub array of $\mathbb{Z}^2$. Similarly a 3D grid $\mathbb{G}$ is either $\mathbb{Z}^3$ or $l \times m \times n$ sub array of $\mathbb{Z}^3$. Therefore, in 2D an $m \times n$ square grid is grid point model can be given as

$$\mathbb{G}_{m,n} = \big\{(i, j) \in \mathbb{Z}^2 : (1 \leqslant i \leqslant m) \wedge (1 \leqslant i \leqslant n\big\}).$$

In the *grid cell model*, a grid vertex is called a 0-cell, a grid edge is a 1-cell, a grid face is a 2-cell, and a grid cube is a 3-cell. A 2D grid $\mathbb{G}$ is either infinite 2-cell or $m \times n$ block of 2-cells whose union $\bigcup\mathbb{G}$ is a rectangular region of euclidean space. Similarly, a 3D grid is either infinite 3-cells or an $l \times m \times n$ set of 3-cells whose union is a cuboid in Euclidean space.

1.1 Simplex Grid

In grid point model, each point is the center of a 2D *pixels* or a 3D *voxels*. Generally *square pixels* are used on square grid and *cubic voxels* are used on cubic grid. All points in the surface of a square pixel or cubic voxel are not equidistant from grid point. However this interesting property exists when we consider the shape of pixels to be circular or voxels to spherical. The choice of pixel and grid is important in digital modeling. Spherical voxels are not stable on cubical grid. The most stable alignment of spheres forms a *tetrahedron* shape, the stability occur due to self alignment of spheres. Tetrahedral grid is*simplex grid* in 3D. A simplex grid is generalization of tetrahedral and triangle grid to n dimensions. For e.g. 2-simplex grid is triangular and 3-simplex grid is tetrahedral. The dual of a grid can be formed by joining the center of adjacent regions formed in the original grid. *Hexagonal grid* is the dual of triangular grid. Dual relation between triangular grid and hexagonal grid is shown in Figure 1.1.

We have used grid point model to analyzes simplex grid in 3D with spherical voxels. *Top view* of a sphere is circle (alternatively we refer to it as a *cell*). By top view we mean the view from a line of sight which is orthogonal to the referenced plane. Top view of tetrahedral grid is shown in Figure 1.2.

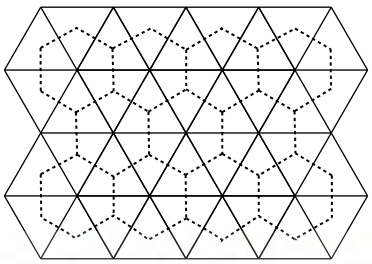

Figure 1.1: Part of a triangular grid is shown in solid lines and its dual hexagonal grid in dashed lines.

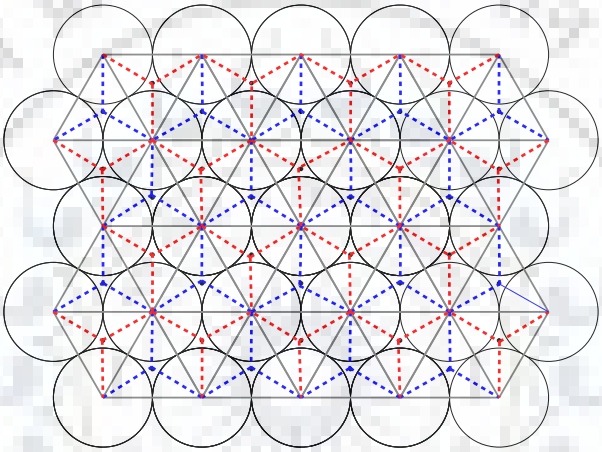

Figure 1.2: Top view of a tetrahedral grid and a layer of spherical voxels on it. Tetrahedron which is represented in dotted blue have their 3 vertices on the same plane and the fourth vertex is above that plane. Similarly, tetrahedron which is represented in dotted red have their 4th vertex below the plane.

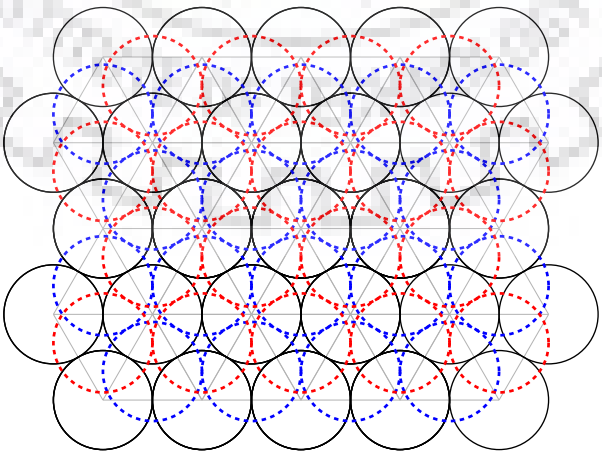

Figure 1.3: Top view of tetrahedral packing of spheres. Spheres in the same plane are represented in solid black and spheres above the plane are represented in dotted blue and spheres that are below the plane are represented in dotted red.

It is clear from Figure 1.2 that adjacent tetrahedron which share an edge have opposite orientation in the sense that fourth vertex is either below the plane or above the plane. Each vertex of a tetrahedron is the center of a sphere. A tetrahedral packing of spheres is shown in Figure 1.3. We can observe that a sphere touches six other spheres on the same plane. It also touches three sphere above the plane and three below the plane. Two spheres are *neighbors* or *connected* to each other if they touches each other. Therefore, each sphere can have at most 12 neighbors on tetrahedral grid. Top view of tetrahedral grid forms a regular triangular grid if we restrict ourselves to some reference plane. Which coincides with one of the parallel planes forming the tetrahedral grid. Therefore it is necessary to study triangular grid to understand tetrahedral grid in details. We analyze triangular grid in section 3 for a possible future extension of the analysis in tetrahedral grid.

1.2 Existing Work

Orthogonal regular grids such as square grid are explored very widely so far due to their natural representation in $\mathbb{Z}^n$. Most graphics applications use square grid. Other regular grid in 2D are triangular and hexagonal grid. Triangular grid is also called as *isometric grid* because set of grid lines intersect one another at an angle of 60°. Hexagonal grid are formed by joining many regular hexagons by their edges. Triangular and hexagonal grid are not addressed in detail because of their non-orthogonal nature. however they do have their own properties which can be used in specific applications. In recent time, a considerable amount of work has been done on triangular and hexagonal grid [1, 15, 16]. Recall that triangular and hexagonal grid are dual of each other as shown in Figure 1.1. They can be interchangeably used based on grid model.

A grid cell model based approach is shown to represent optimal polygon to address isoperimetric problem in [15]. The method determines the geometric objects that have maximum area among same perimeter objects and also makes sure the objects have minimum perimeter among those that have least area. They have used 4 and 8-neighborhood properties of square grid to introduce their previous results on square grid. The 3-coordinate system is used to represent triangular grid with odd or even grid points due to two different orientations of triangles. They have formulated the perimeter and area of optimal object with polygon side length as a parameter.

Euclidean circle approximation by neighborhood sequence on hexagonal grid (represented by grid point model) is presented in [16]. A classification of digital circle is done based on their digital distance. The digital distance is calculated by the neighboring sequence. Based on this sequence, digital circles are characterized. Best approximations are used for small circles and a greedy approach is given for larger circles which results in fast approximation. Three types of neighbors are defined for a grid point. A state transition is presented with neighboring sequence as input parameter and type of digital circle formed as states. The parameter and area of approximated digital circle is formulated in term of side length of polygon formed. Non-compactness ratio parameter is used to compare best approximation for small circles. 3-coordinate system is used to represent point on grid, their relation to Cartesian 2-coordinate system is required to calculate area and perimeter.

Digital circle characterization on triangular grid for grid cell model is presented in [14] by general neighborhood sequence that define digital circle with formation of waveform . The neighborhood sequence represent a waveform which grows as we move away from the center of the circle. The development of changing of waveform plays important role in representation of digital circle. 3-coordinate system is used with three types of neighborhood. A hierarchical digital circle transition is shown as states with neighborhood sequence. Two or more neighborhood sequences may grow into the same circle representation with different waveform formation in their intermediate stage. Different type of waveform is presented with relation between them by neighborhood sequence. A relation to neighborhood sequence, waveform shape and polygon formed by digital circle has been discussed.

Construction of minimum-area geometric cover of digital object is presented in [1] on the triangular grid (represented by grid point model). It use the triangle cover of objects on the grid. 3-coordinate system is used that divides the grid into six sextants. Grid points are classified based on triangular cover around it. Determination of next direction plays important role in algorithm to construct triangular cover. The complexity of the algorithm is given in terms of grid size and pixel size that border a connected component. Experimental results are shown for objects on different grid size. The algorithm presented constructs triangular cover for digital object with multiple components and holes.

1.3 Our Contribution

While triangular and hexagonal grid are addressed considerably, simplex grid in general or in 3D is not address up to considerable level. In this report, we will try to explore simplex grid by using triangular grid which is 2-simplex. This analysis is expected to assist us in our future transition to tetrahedral grid which is 3-simplex. Most of the work uses neighborhood relation of grid points. We will also exploit the neighborhood properties on simplex grid in a coherent manner. A consistent 3-coordinate system is used to represent grid points on 2D plane which motivates us to use the same system in our representation. We will restrict ourselves to integer based approaches during analysis of geometric objects as it is efficient in terms of computation and also leads to accurate results by avoiding round-off errors associated with floating point operations.

The report has been organized as follows. We first introduce some theoretical framework of our work in section 2. section 3 deals with our first contribution on Euclidean distance formula for three coordinate system, cell type notation, the relation between cell type and coordinate system, and geometric objects representation namely digital lines, digital circle, and arcs on the triangular grid. In section 4, we have introduced the four coordinate system which is an extension of three coordinate system described in section 3. section 5 deals with the representation of geometric objects namely sphere, digital plane, and tetrahedron. We conclude our work in section 6 by giving the application and advantages of our work.

2 Theoretical Foundation

A *regular simplex grid* in 2D is a set of equilateral triangles that are connected by their common edges or corners. Their corners are called grid points which are the center of circular pixels (we refer circular pixels as cells from now on). A grid point is represented by coordinates in $\mathbb{Z}^2$ or $\mathbb{Z}^3$. In the square grid, it is simple to represent a grid point by (x, y) coordinates in which x- and y-axes divide the plane into four quadrants. A point $(i,\ j)$ on square grid have four neighbors given by $(i \pm 1,\ j)$ and $(i,\ j \pm 1)$. Two grid points are called as *direct neighbors* if there exists a grid edge between them. The simplex grid is not uniform in the sense that two different orientations of the triangles occur, Therefore so we need an integer based coordinate system which is different from the square grid. A 2 coordinate system is introduced in [11] in which odd-numbered rows of a Cartesian grid is shifted $\frac{1}{2}$ unit distance to the right. That is equivalent to working with an unsifted Cartesian grid, but treating a point $(i,\ j)$ on an odd-numbered row as having the six neighbors $(i \pm 1,\ j)$, $(i,\ j \pm 1)$ and $(i+1,\ j \pm 1)$, while a point on an even-numbered row has the six neighbors $(i \pm 1,\ j)$, $(i,\ j \pm 1)$ and $(i-1,\ j \pm 1)$. which leads to inconsistency with respect to the random grid point.

2.1 Regular Simplex Grid Representation

We have introduced the consistent coordinate system in the same way, as it was given in [4]. For nodes of the triangular grid, the grid intersection point are considered as grid points and three coordinate values are assigned to each of them. The following procedure helps in assigning the coordinates.

A grid point is chosen as origin and assigned coordinate values as $(0,\ 0,\ 0)$. Then we fix three coordinate axes around it. The direction of the $x-$, $y-$ and $z-$axes are taken as 0°, 120° and 240°, respectively [13] as shown in Figure 2.1. These axes divide the grid around origin into 6 equal regions called as *sextant* and the $x-$, $y-$, $z-$axes are called as *sextant axes*. Other grid points coordinate values are inductively assigned. If the coordinates of a random point on the grid are $(a1,\ a2,\ a3)$, then the coordinates of its neighbor in the positive x-direction are $(a1+1,\ a2,\ a3-1)$, and in the negative x-direction are $(a1-1,\ a2,\ a3+1)$. Similarly, in the positive y-direction, we get $(a1-1,\ a2+1,\ a3)$, and in the negative y-direction we get $(a1+1,\ a2-1,\ a3)$. The coordinate values in the positive z-direction are $(a1,\ a2-1,\ a3+1)$, and in the negative z-direction are $(a1,\ a2-1,\ a3+1)$.

Note that in this representation the sum of the coordinate values of every point is 0. Two points are direct neighbors if any of their coordinate value is the same, and the differences of the other two corresponding coordinate values are ± 1. The grid can be divided into sextants around a random point other than origin by following the same procedure as described above considering the new chosen point as origin. This point is called as *base point*. The direct neighbors in the 3-coordinate system are shown for a random base point in Figure 2.2. The $z-$axis can be represented by equation $x = 0$ similarly $y-$axis by $z = 0$ and $x-$axis by $y = 0$ as their respective values on the given axis is always zero.

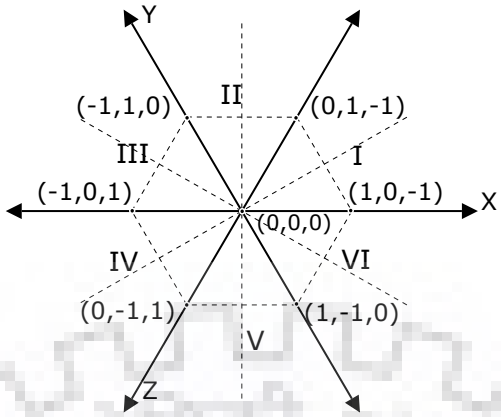

Figure 2.1: 3-coordinate system for triangular grid showing neighbors of the grid point $(0, \ ,0 \ ,0)$ and the six sextants.

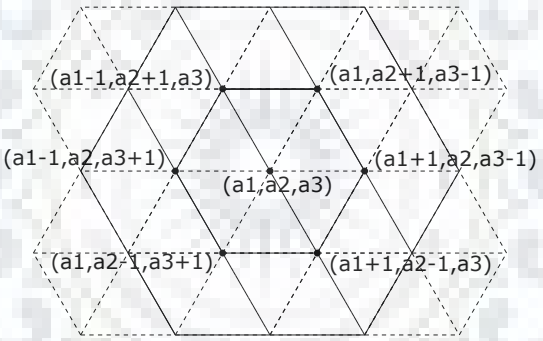

Figure 2.2: Neighbors of a random point on a 3-coordinate system.

The properties of the the triangular grid are as follows.

1. Triangular grid has the higher degree of symmetry than the orthogonal grid.
2. Each point in the Triangular grid have six direct neighboring point each at unit distance in 0°, 60°, 120°, 180°, 240°, 300° direction respectively.
3. Hexagonal grid is dual of the triangular grid and can be interchangeably used based on grid model.

The properties of the three coordinate system are as follows.

1. The triangular grid is divided into six sextants around a point.
2. Each sextant is divided into two symmetrical halves known as *duo-decant*.

3. Each point $(x,\ y,\ z)$ satisfy following equation [4].

$$x+y+z=0.$$

4. Neighbors of a point $(x,\ ,y\ ,z)$ are $(x+1,\ y,\ z-1,\ w)$, $(x-1,\ y,\ z+1,\ w)$, $(x-1,\ y+1,\ z,\ w)$, $(x,\ y+1,\ z-1,\ w)$, $(x,\ y-1,\ z+1,\ w)$ and $(x+1,\ y-1,\ z,\ w)$ [4].

5. Every point $(x,\ ,y\ ,z)$ have twelve symmetric points including itself. These are $(x,\ y,\ z)$, $(y,\ x,\ z)$, $(-y,\ -z,\ -x)$, $(-x,\ -z,\ -y)$, $(z,\ x,\ y)$, $(z,\ y,\ x)$, $(-x,\ -y,\ -z)$, $(-y,\ -x,\ -z)$, $(y,\ z,\ x)$, $(x,\ z,\ y)$, $(-z,\ -x,\ -y)$,$(-z,\ -y,\ -x)$[4] in each duo-decant.

6. Transformation such as rotation, translation, Reflection can be performed.

7. It can be extended to four coordinate system for tetrahedral grid.

Theorem 1. The sum of coordinate values of every point $(x,\ y,\ z)$ is zero.

$$\forall \text{ points}(x,\ y,\ z)\ x+y+z=0.$$

Proof. It is trivially valid for origin $(0,\ 0,\ 0)$. Now we consider the neighbors of origin as $(1,\ 0,\ -1)$, $(0,\ 1,\ -1)$, $(-1,\ 1,\ 0)$, $(-1,\ 0,\ 1)$, $(0,\ -1,\ 1)$, $(1,\ -1,\ 0)$. Their sum of coordinate value is also zero. Similarly, direct neighbors of these points also satisfy the equation and so on. □

Alternate proof. Proof by Induction. P(0): is true for $(0,\ 0,\ 0)$.

P(1): is true for all direct neighbors of $(0,\ 0,\ 0)$.

Let P(n) be true for $(x_n,\ y_n,\ z_n)$

$$x_n+y_n+z_n=0.$$

direct neighbors of $(x_n,\ y_n,\ z_n)$ are $(x_n+1,\ y_n,\ z_n-1)$, $(x_n,\ y_n+1,\ z_n-1)$, $(x_n-1,\ y_n+1,\ z_n)$, $(x_n-1,\ y_n,\ z_n+1)$, $(0,\ y_n-1,\ z_n+1)$, $(x_n+1,\ y_n-1,\ z_n)$ also satisfy the equation. This shows that P(n+1) is true. This concludes our inductive step. □

Corollary 1. A point is a valid grid point if and only if the sum of its coordinate value is zero and every coordinate value is an integer.

3 Three Coordinate System on Triangular Grid

In this section, we will analyze the three coordinate system and represent geometric objects on the triangular grid.

3.1 Euclidean Distance between Cells

By the formal definition, two circular cells are *direct neighbors* if they touch each other, In terms of the grid point, two circular cells are direct neighbor if there exists a grid edge between their center (grid points). Circular cells are simply referred as *cells* in our discussion. we can easily prove that every cell has six direct neighbors. We call these direct neighbors as level-1 neighbors. Let us consider the size of the equilateral triangle that forms the regular simplex grid is d, the diameter of the cell is also d. It is clear from Figure 2.2 that distance between direct neighbors is d. *Grid distance* between two cells is defined as the minimum number of steps required to reach from one cell to another along the direction of sextant axes. We define *level* for a cell around a base cell as grid distance from the base cell. All cells which are at same grid distance from a base cell at the same level. n^{th} level neighbors for a cell is defined as the direct neighbors of $(n-1)^{th}$ level in the outward direction from the base cell. In this way, we can say level-2 cells are direct neighbors of the level-1 cell.

Consider a cell at random point. It has six direct neighbors at level-1. We are interested in calculating the Euclidean distance for different levels. All cells at level 1 around base cell form a hexagonal structure which can be observed for level 1 and level 2 in Figure 2.2. The sextant axes divide the grid into 6 symmetric sextants. Therefore we only need to calculate the Euclidean distance in one of the sextants. Let us consider n as the number of levels. Now we need to calculate euclidean distance only in one of the sextants for n^{th} level. for level-1, $n = 1$, distance$= d$ and total neighbors$= 6$. Furthermore, a sextant is dived into two symmetrical halves around a base cell as shown by the dotted line in Figure 3.1.

We define a parameter t for a level n as the number of cells that do not lie at sextant axes in a symmetrical half of a sextant. If a cell partially (half-cell) lies inside the symmetrical half, it is counted as one complete cell.

$$t = \begin{cases} \frac{n}{2} & \text{if n is even} \\ \frac{n-1}{2} & \text{if n is odd} \end{cases} \tag{3.1}$$

It can be easily shown by induction that parameter t always satisfies the Equation 3.1. For n=1, we get t=0, as there are no other neighbors other than six direct neighbors which are at integer distance d. We have introduced a Notation $T_{i,j}$ for cells where j represent the level of the cell from the base cell and i is the number assigned to the cell in the following way. Cells at level j around a base point in a symmetrical half are numbered from 0 to $t-1$ starting from the line (that partition the sextant) toward sextant axes. The cell that lies at sextant axes is numbered as t. Trivially $T_{0,0}$ is base cell itself. Its direct neighbor is $T_{0,1}$. We define $D(T_{i,j})$ as the euclidean

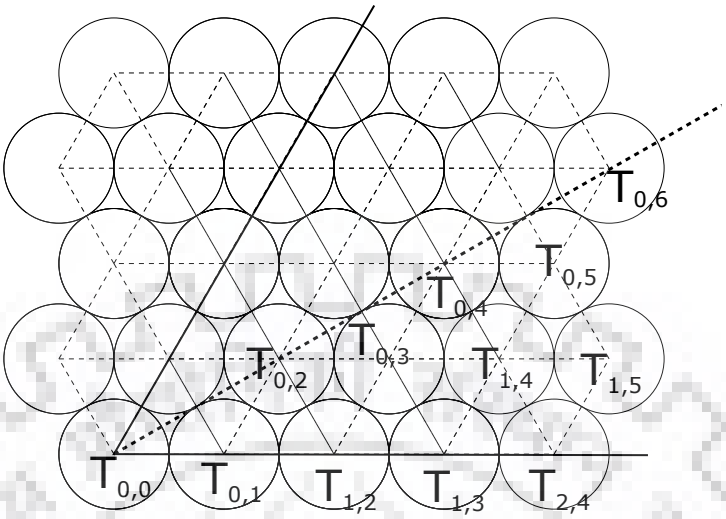

Figure 3.1: Type of cells.

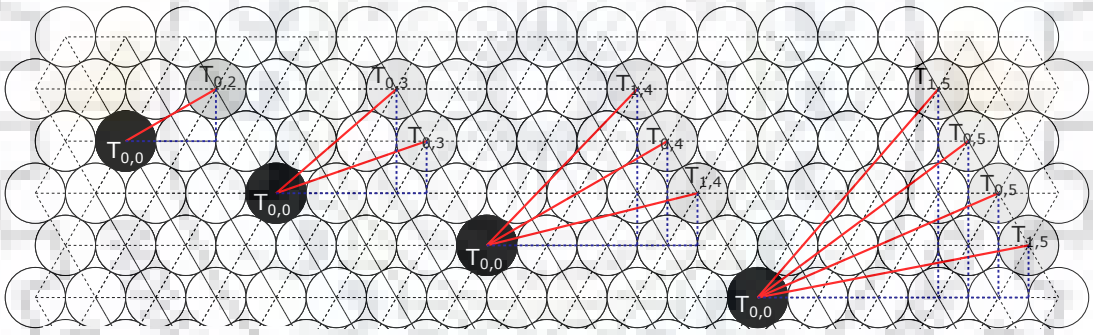

Figure 3.2: Distance of cells at different levels.

distance of cell $T_{i,j}$ from cell $T_{0,0}$ (i.e base cell). Following relations always hold.

1. Cell $T_{t,n}$ is always at integer distance as shown in Figure 3.1. $D(T_{t,n}) = nd$
2. Cell $T_{i,n}$ may or may not be at integer distance and $D(T_{i,n}) < D(T_{t,n})$ where $i = [0, t-1]$
3. If n is even, number of cells of type $T_{0,n}$ in a sextant is 1. The dotted line passes through them as shown in Figure 3.1 and for $i = [1, t-1]$ number of cell of type $T_{i,n}$ is two. one in each symmetrical half.
4. If n is odd, number of cell of type $T_{i,n}$ in a sextant is two for $i = [0, t-1]$.

Next we aim to find the $D(T_{i,n})$ for $i = [0, t-1]$, we know that,

$$D(T_{0,1}) = d, \qquad D(T_{1,2}) = 2d, \qquad D(T_{1,3}) = 3d \qquad \text{because} \qquad D(T_{t,n}) = nd.$$

Similarly,

$$D(T_{2,4}) = 4d, \qquad D(T_{2,5}) = 5d, \qquad D(T_{3,6}) = 6d, \qquad D(T_{3,7}) = 7d.$$

Refer to Figure 3.2 for a visualization of these distances
For $n = 2, t = 1, i = [0,0] = 0$, we get

$$D(T_{0,2}) = \sqrt{\left(\frac{3d}{2}\right)^2 + \left(\frac{\sqrt{3}d}{2}\right)^2} = \sqrt{3}d.$$

For $n = 3, t = 1, i = [0,0] = 0$,

$$D(T_{0,3}) = \sqrt{\left(\frac{5d}{2}\right)^2 + \left(\frac{\sqrt{3}d}{2}\right)^2} = \sqrt{7}d.$$

For $n = 4, t = 2, i = [0,1]$,

$$D(T_{0,4}) = \sqrt{(3d)^2 + \left(\sqrt{3}d\right)^2} = \sqrt{12}d \qquad D(T_{1,4}) = \sqrt{\left(\frac{7d}{2}\right)^2 + \left(\frac{\sqrt{3}d}{2}\right)^2} = \sqrt{13}d.$$

For $n = 5, t = 2, i = [0,1]$,

$$D(T_{0,5}) = \sqrt{(4d)^2 + \left(\sqrt{3}d\right)^2} = \sqrt{19}d \qquad D(T_{1,5}) = \sqrt{\left(\frac{9d}{2}\right)^2 + \left(\frac{\sqrt{3}d}{2}\right)^2} = \sqrt{21}.$$

Similarly, For $n = 6, t = 3, i = [0,2]$,

$$D(T_{0,6}) = \sqrt{27}d, \qquad D(T_{1,6}) = \sqrt{28}d, \qquad D(T_{2,6}) = \sqrt{31}d.$$

For $n = 7, t = 3, i = [0,2]$,

$$D(T_{0,7}) = \sqrt{37}d, \qquad D(T_{1,7}) = \sqrt{39}d, \qquad D(T_{2,7}) = \sqrt{43}d.$$

For $n = 8, t = 4, i = [0,3]$,

$$D(T_{0,8}) = \sqrt{48}d, \qquad D(T_{1,8}) = \sqrt{49}d = 7d, \qquad D(T_{2,8}) = \sqrt{52}d, \qquad D(T_{3,8}) = \sqrt{57}d.$$

For $n = 9, t = 4, i = [0,3]$,

$$D(T_{0,9}) = \sqrt{61}d, \qquad D(T_{1,9}) = \sqrt{63}d, \qquad D(T_{2,9}) = \sqrt{67}d, \qquad D(T_{3,9}) = \sqrt{73}d.$$

Table 3.1: Horizontal and vertical distance of a cell form base cell.

i	h	v
0	$n-\frac{1}{2}(t)$	$t\frac{\sqrt{3}}{2}$
1	$n-\frac{1}{2}(t-1)$	$(t-1)\frac{\sqrt{3}}{2}$
2	$n-\frac{1}{2}(t-2)$	$(t-2)\frac{\sqrt{3}}{2}$
...	...	...
t-1	$n-\frac{1}{2}$	$\frac{\sqrt{3}}{2}$

For level n, $t=\lfloor\frac{n}{2}\rfloor$ as defined in Equation 3.1. Therefore we get that $D(T_{i,n})=d\sqrt{h^2+v^2}$ where h,v are horizontal and vertical distance of cell $T_{i,n}$ from base cell respectively as given in Table 3.1 in terms of n, t and i.

This lead to generalization of $D(T_{i,n})$ as

$$D(T_{i,n})=d\sqrt{\left[n-\frac{1}{2}(t-i)\right]^2+\left[\frac{\sqrt{3}}{2}(t-i)\right]^2} \tag{3.2}$$

Putting value of t in Equation 3.2 from Equation 3.1, we get

$$D(T_{i,n})=\begin{cases} d\sqrt{\frac{3}{4}n^2+i^2} & \text{if n is even and } 0\le i\le\frac{n}{2} \\ d\sqrt{\frac{3}{4}n^2+i^2+i+\frac{1}{4}} & \text{if n is odd and } 0\le i\le\frac{n-1}{2} \end{cases} \tag{3.3}$$

We have observed that for $n=8$ and $i=1$, $D(T_{1,8})=7d$, which is the smallest possible value of n and i for which $D(T_{i,n})$ is an integer.

3.2 Relation between 3-Coordinate System and Cell Types

A point $p(a1,\ a2,\ a3)$ is in sextant-I with reference to origin $(0,\ 0,\ 0)$ if and only if $|a1+a2|=|a3|$ and $a3<0$, similarly p is in sextant-IV if and only if $|a1+a2|=|a3|$ and $a3>0$ For a point $p(a1,\ a2,\ a3)$ sextant conditions are summarized in Table 3.2

Table 3.2: Sextant condition.

Sextant	condition
I	$\lvert a1+a2\rvert=\lvert a3\rvert$ and $a3<0$
II	$\lvert a1+a3\rvert=\lvert a2\rvert$ and $a2>0$
III	$\lvert a2+a3\rvert=\lvert a1\rvert$ and $a1<0$
IV	$\lvert a1+a2\rvert=\lvert a3\rvert$ and $a3>0$
V	$\lvert a1+a3\rvert=\lvert a2\rvert$ and $a2<0$
VI	$\lvert a2+a3\rvert=\lvert a1\rvert$ and $a1>0$

A point $p(a1,\ a2,\ a3)$ in sextant-I is the center of cell of type $T_{i,j}$ where $j = |a3|$ and

$$i = \frac{|a1-a2|}{2} \quad \text{if } j \text{ is even} \qquad i = \frac{|a1-a2|-1}{2} \quad \text{if } j \text{ is odd}$$

For example, point $p(4,\ 2,\ -6)$ is the center of cell $T_{1,6}$. $i = \frac{|4-2|}{2} = 1,\ j = |-6| = 6$ and point $p(1,\ 4,\ -5)$ is the center of cell $T_{1,5}$. $i = \frac{|1-4|-1}{2} = 1,\ j = |-5| = 5$.

Table 3.3: Determination of cell types and levels from cell coordinate $(a1,\ a2,\ a3)$.

Sextant	i (Type)	j (Level)
I,IV	$\frac{\lvert a1-a2\rvert}{2}$, if $\lvert a3\rvert$ is even $\frac{\lvert a1-a2\rvert-1}{2}$, if $\lvert a3\rvert$ is odd	$\lvert a3\rvert$
II,V	$\frac{\lvert a1-a3\rvert}{2}$, if $\lvert a2\rvert$ is even $\frac{\lvert a1-a3\rvert-1}{2}$, if $\lvert a2\rvert$ is odd	$\lvert a2\rvert$
III,VI	$\frac{\lvert a2-a3\rvert}{2}$, if $\lvert a1\rvert$ is even $\frac{\lvert a2-a3\rvert-1}{2}$, if $\lvert a1\rvert$ is odd	$\lvert a1\rvert$

Similarly, we can get the cell $T_{i,j}$, when its center point $p(a1,\ a2,\ a3)$ is given. The value of i and j can be determined by Table 3.3.

For a given cell $T_{i,j}$, its coordinates value can be determined from Table 3.4. The special case when $i = 0$ and j is even, there is only one cell of type $T_{0,j}$ in each sextant whose coordinates can be determined from Table 3.5 as it was counted twice in the definition of t for each symmetrical half.

Table 3.5: Coordinates value from cell type when $i = 0$ and j (Level) is even.

Sextant	Coordinates
I	$\left(\frac{j}{2},\ \frac{j}{2},\ -j\right)$
IV	$\left(-\frac{j}{2},\ -\frac{j}{2},\ j\right)$
II	$\left(-\frac{j}{2},\ j,\ -\frac{j}{2}\right)$
V	$\left(\frac{j}{2},\ -j,\ \frac{j}{2}\right)$
III	$\left(-j,\ \frac{j}{2},\ \frac{j}{2}\right)$
VI	$\left(j,\ -\frac{j}{2},\ -\frac{j}{2}\right)$

Table 3.4: Coordinate values from cell type $T_{i,j}$.

Sextant	j (level)	Coordinates
I	if j is even	$\left(\frac{j+2i}{2}, \frac{j-2i}{2}, -j\right), \left(\frac{j-2i}{2}, \frac{j+2i}{2}, -j\right)$
	if j is odd	$\left(\frac{j+2i+1}{2}, \frac{j-2i-1}{2}, -j\right), \left(\frac{j-2i-1}{2}, \frac{j+2i+1}{2}, -j\right)$
IV	if j is even	$\left(\frac{j+2i}{2}, \frac{j-2i}{2}, j\right), \left(\frac{j-2i}{2}, \frac{j+2i}{2}, j\right)$
	if j is odd	$\left(\frac{j+2i+1}{2}, \frac{j-2i-1}{2}, j\right), \left(\frac{j-2i-1}{2}, \frac{j+2i+1}{2}, j\right)$
II	if j is even	$\left(\frac{j+2i}{2}, j, \frac{j-2i}{2}\right), \left(\frac{j-2i}{2}, j, \frac{j+2i}{2}\right)$
	if j is odd	$\left(\frac{j+2i+1}{2}, j, \frac{j-2i-1}{2}\right), \left(\frac{j-2i-1}{2}, j, \frac{j+2i+1}{2}\right)$
V	if j is even	$\left(\frac{j+2i}{2}, -j, \frac{j-2i}{2}\right), \left(\frac{j-2i}{2}, -j, \frac{j+2i}{2}\right)$
	if j is odd	$\left(\frac{j+2i+1}{2}, -j, \frac{j-2i-1}{2}\right), \left(\frac{j-2i-1}{2}, -j, \frac{j+2i+1}{2}\right)$
III	if j is even	$\left(-j, \frac{j+2i}{2}, \frac{j-2i}{2}\right), \left(-j, \frac{j-2i}{2}, \frac{j+2i}{2}\right)$
	if j is odd	$\left(-j, \frac{j+2i+1}{2}, \frac{j-2i-1}{2}\right), \left(-j, \frac{j-2i-1}{2}, \frac{j+2i+1}{2}\right)$
VI	if j is even	$\left(j, \frac{j+2i}{2}, \frac{j-2i}{2}\right), \left(j, \frac{j-2i}{2}, \frac{j+2i}{2}\right)$
	if j is odd	$\left(j, \frac{j+2i+1}{2}, \frac{j-2i-1}{2}\right), \left(j, \frac{j-2i-1}{2}, \frac{j+2i+1}{2}\right)$

3.3 Representation of Geometric Objects

In this section, we describe the basic geometric objects namely digital line, digital circle, and digital arc on the simplex grid.

Digital Line

Digital lines in the simplex grid can be obtained by an algorithm. The algorithm is optimum straight-line approximation with direction constrained as unit distance movement in any one of the six possible directions. A modified Bresenham algorithm is presented in [2] for the 2-coordinate system for a triangular grid. We have introduced the concept of cell type $T_{i,j}$ for the 3-coordinate system and its relation to coordinate values. There is six possible unit distance movement for a given cell. As we have shown in the previous section that a sextant can be divided into two symmetrical halves. We call them left and the right symmetrical half around a base point as given in Table 3.6. Similarly, for other sextants these conditions satisfy with necessary changes in coordinate comparison, therefore so we can say that grid is divided into 12 *symmetrical sectors* around a base point. Our focus will be on one of those sectors. We choose right symmetrical half in our discussion. We have proposed two ways to generate the straight line for the 3-coordinate system.

Table 3.6: Position of cell $(x,\ y,\ z)$ in sextant I with respect to base cell.

condition	position
$x < y$	left symmetrical half
$x > y$	right symmetrical half
$x = y$	on the partition line

Given two point $p_1(x_1,\ y_1,\ z_1)$ and $p_2(x_2,\ y_2,\ z_2)$. One of the these points is chosen as base point. Let p_1 is selected as base point $(x_r,\ y_r,\ z_r)$ where $(x_r,\ y_r,\ z_r) = (x_1,\ y_1,\ z_1)$, then the other point will be $(x_2 - x_r,\ y_2 - y_r,\ z_2 - z_r)$ with respect to the base point. Point p_1 will be at origin with respect to base point (i.e. itself) and point p_2 position in term of sextant will be determined by Table 3.2. Let us assume that point p_2 lies in right symmetrical half in sextant-I. We can say that we have to find the shortest path from origin to point $p_2(x_2 - x_r,\ y_2 - y_r,\ z_2 - z_r)$ using the two possible direction movements. Value of $|Z|$=($|z_2 - z_r|$) is level or length of the path, and in every step current cell $C(x,\ y,\ z)$ have next possible cells $A(x,\ y+1,\ z-1)$ and $B(x+1,\ y,\ z-1)$. The determination of next cell from current cell depends on the difference between perpendicular distance from the center of next possible cells to line, as shown in Figure 3.3.For current cell $C(x,\ y,\ z)$ in sextant-I,

$$\begin{aligned} &\text{If } AP - QB < 0 \qquad \text{cell } A(x,\ y+1,\ z-1) \text{ is next cell,} \\ &\text{If } AP - QB \geq 0 \qquad \text{cell } B(x+1,\ y,\ z-1) \text{ is next cell.} \end{aligned}$$

The constraint is that we only know the cell coordinates and we restrict ourselves in integer domain to ensure the obvious advantages. The decision parameter value $AP - QB$ precisely determine the next cell. Challenge is to find the equivalent integer based parameters.

Other approach is based on partitioning of line into segments which heavily depends on the partitioning method. As we know, $|Z|$ gives the level in sextant I. We compare the value of other two coordinate x and y and find out the minimum value, the coordinate value x gives us the number of times direction changes to reach $(x+1,\ y,\ z-1)$ from $(x,\ y,\ z)$ and similarly coordinate value y gives number of times the direction changes to reach $(x,\ y+1,\ z-1)$ from $(x,\ y,\ z)$. If we can determine those points where the direction changes (shown in dark in Figure 3.4), we can partition the line into smaller segments which coincides with segments of grid lines and can be easily drawn on the grid. Figure 3.4 shows the partitioning of a line into segments.

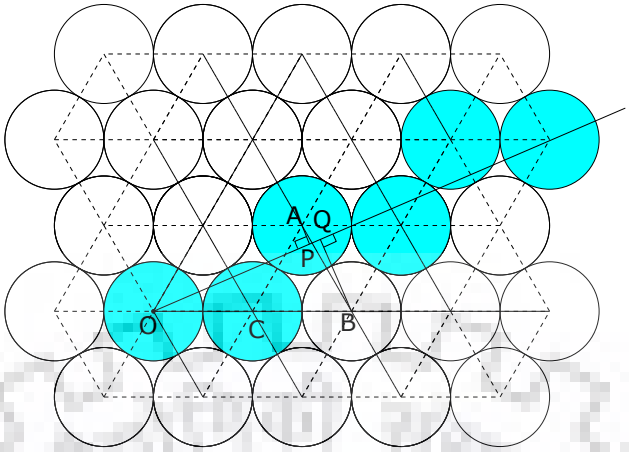

Figure 3.3: Determination of next cell in sextant I by the sign of $AP - QB$, where A and B are next possible cells from current cell C with respect to reference cell O. Perpendicular is drawn on the line from cell A and B meet at P and Q respectively.

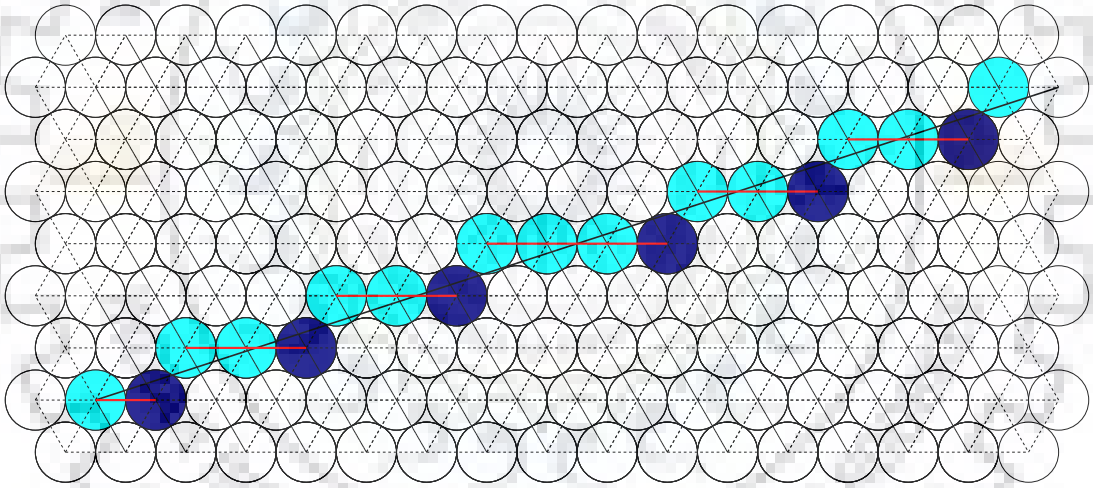

Figure 3.4: Partitioning of the line into Segments. Cells at which direction changes are shown in dark.

Digital Circle

The algorithm to produce digital circle is presented in [17] for the 2-coordinate system which is closely related to [2]. Our concern is to propose the similar approach in the 3-coordinate system. As we know, the grid is divided into 12 symmetric sectors around a base cell. The center of the digital circle is selected as base cell around which this partitioning is done. If we calculate coordinate in any one of those sectors we can easily draw the circle by the symmetry of cell points in other sectors. Given a center cell of $p(x1, y1, z1)$ with radius r, we consider the center cell as our base point. Partitioning of a circle into sectors is shown in Figure 3.5. The symmetry of circle points is shown in Table 3.7.

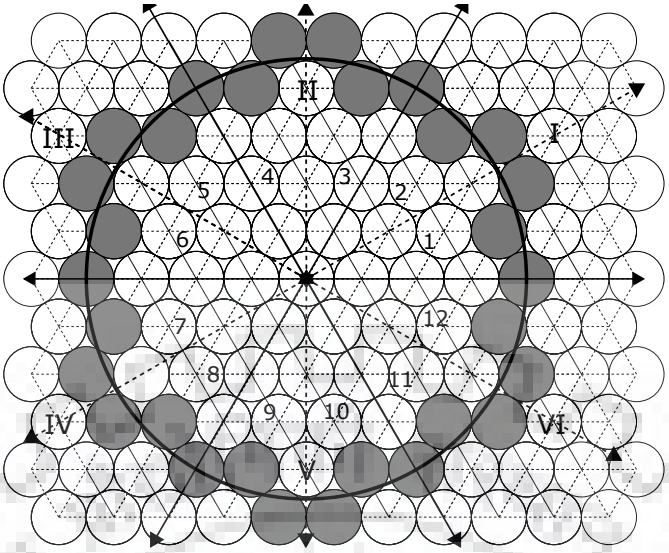

Figure 3.5: Partitioning of the circle into 12 sectors

Table 3.7: Symmetry of cell in 12 sectors of a digital circle.

sector	cell coordinates
c1	$(x,\ y,\ z)$
c2	$(y,\ x,\ z)$
c3	$(-y,\ -z,\ -x)$
c4	$(-x,\ -z,\ -y)$
c5	$(z,\ x,\ y)$
c6	$(z,\ y,\ x)$
c7	$(-x,\ -y,\ -z)$
c8	$(-y,\ -x,\ -z)$
c9	$(y,\ z,\ x)$
c10	$(x,\ z,\ y)$
c11	$(-z,\ -x,\ -y)$
c12	$(-z,\ -y,\ -x)$

Grid Intersection Digitization Model

Digital lines and digital circles are obviously not appropriate to represent random arcs or curves. We need some other representation for curves or arc. We will define grid-intersection digitization in the same way as it was given in [9].

The grid-intersection digitization R(γ) of a planar curve or arc γ is the set of all grid points $(i,\ j,\ k)$ that are closest (in Euclidean distance) to the intersection points of γ with the grid lines.

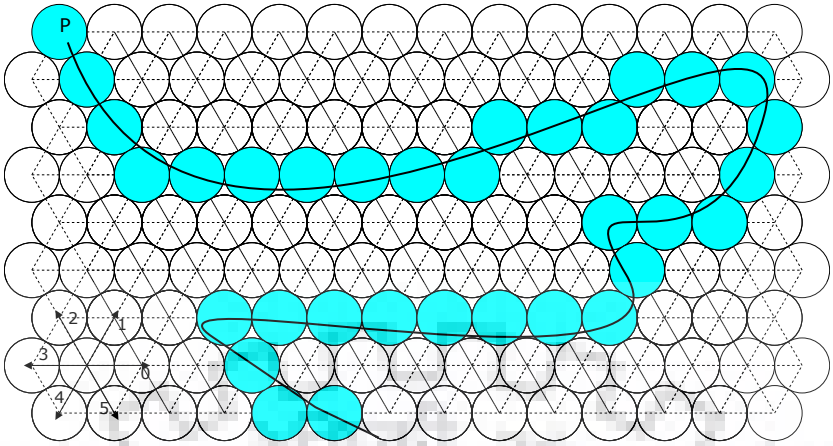

Figure 3.6: Representation of an arc that Starts at p with directional chain as 5550000001...3550.

It is possible that an intersection point may have the same minimum distance to two different grid points, in that case, we choose the rightmost or lowermost point with respect to the arc.

A traversal of R(γ) defines an ordered sequence (list) of grid points in R(γ). The ordered sequence of cell points is called the digitized grid intersection sequence $\rho(\gamma)$ of γ.

If a given R(γ) is tangent to two cells we list only the cell that is below or right of R(γ). The ordered sequence of an arc is shown in Figure 3.6. It defines the chain of grid cell points. The (geometric) length of $\rho(\gamma)$ is the sum of the lengths of the steps. This digitization model can be extended to 3D where we look for the intersection of R(γ) with spherical voxels. A sample arc is shown in Figure 3.6 with start point and directional chain.

4 Four Coordinate System on Tetrahedral Grid

We have represented a single layer of the tetrahedral grid by three coordinates. Similarly, we can represent other layers by three coordinates with the addition of the fourth coordinate that will represent the layer on the tetrahedral grid. We required to represent one of the voxels at other layers with respect to the origin. Other voxels on a particular layer can be represented in the same way as it was described for three coordinate system. Part of a tetrahedral grid is shown in Figure 4.1.

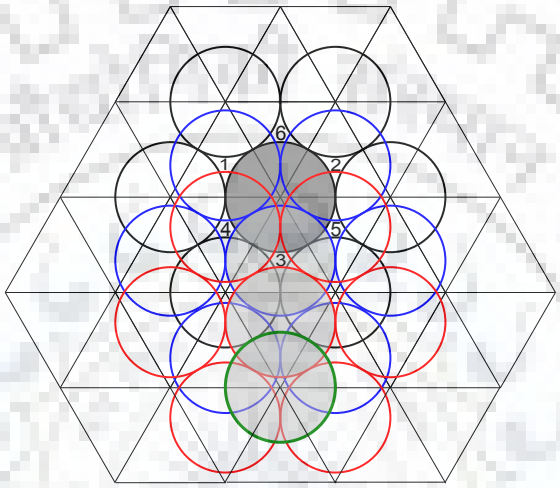

Figure 4.1: Top view of part of a Tetrahedral Grid. Grid lines of the reference plane i.e. layer 0 are represented by black. The sphere at layer 0 is represented by circles of black color. Blue, red and green colored circles respectively represent layer 1, 2 and 3 spheres.

Sphere at origin is shown as dark gray whose coordinates are $(0,\ 0,\ 0,\ 0)$. There are 2 possibility of putting sphere above layer 0. You can either place spheres at position $1-3$ or $4-6$. We have chosen position $1-3$ for upper layer with respect to lower layer in our representation. We can represent any one of the sphere at position $1-3$ above layer 0 by $(0,\ 0,\ 0,\ 1)$. We have chosen position 3 with respect to the origin $(0,\ 0,\ 0,\ 0)$ for coordinate value $(0,\ 0,\ 0,\ 1)$. The fourth coordinate value represent the layer with respect to the reference plane. Now we can represent other layer 1 voxels in the same way as it was described for three coordinate with the addition of fourth coordinate which is always same for a given layer. Similarly, we have put sphere at position $1-3$ on layer 2 with respect to layer 1 which is represented by red colored circles. It is Important to note that we have explicitly represented position $1-6$ with respect to layer 0. Position for the upper layer with respect to the lower layer is directly represented by circles. Red colored circle which is filled by light gray at layer 2 is represented by coordinate value $(0,\ 0,\ 0,\ 2)$.

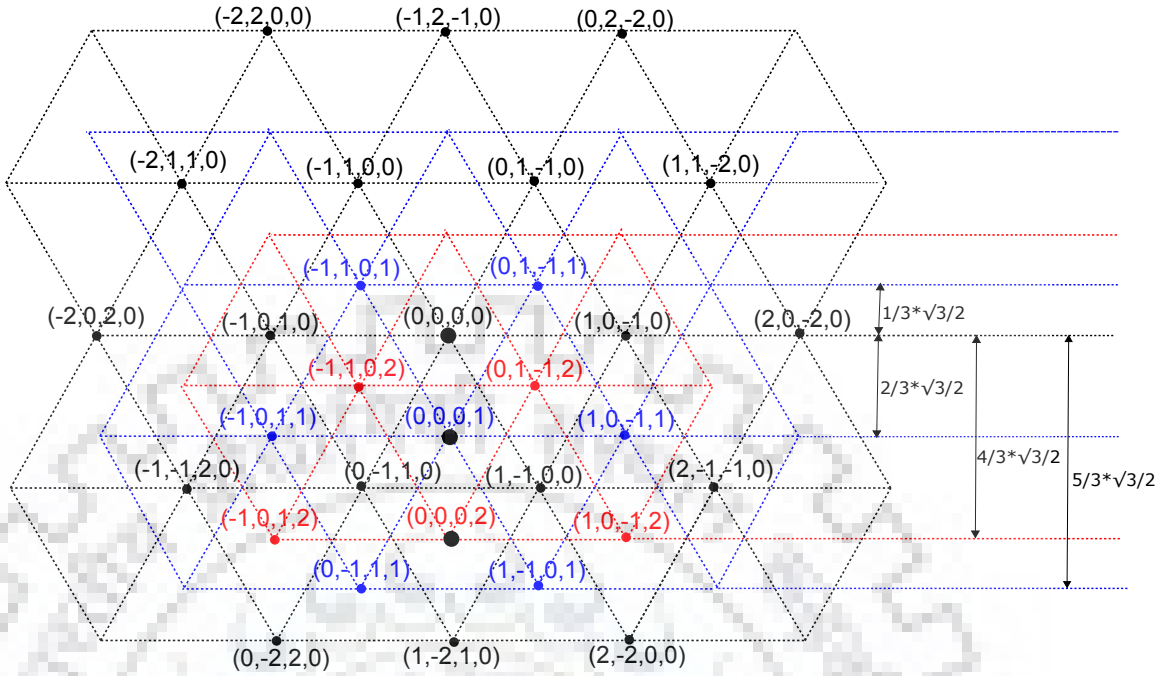

Figure 4.2: Four coordinates system representation. Layer 0, 1, 2 coordinates are represented by black, blue, red color respectively. The distance of the centroid from a vertex is $\frac{2}{3}$ of the height. Centroid divides the perpendicular bisector in 2 : 1 ratio. Height of triangle is $\frac{\sqrt{3}}{2}$ unit.

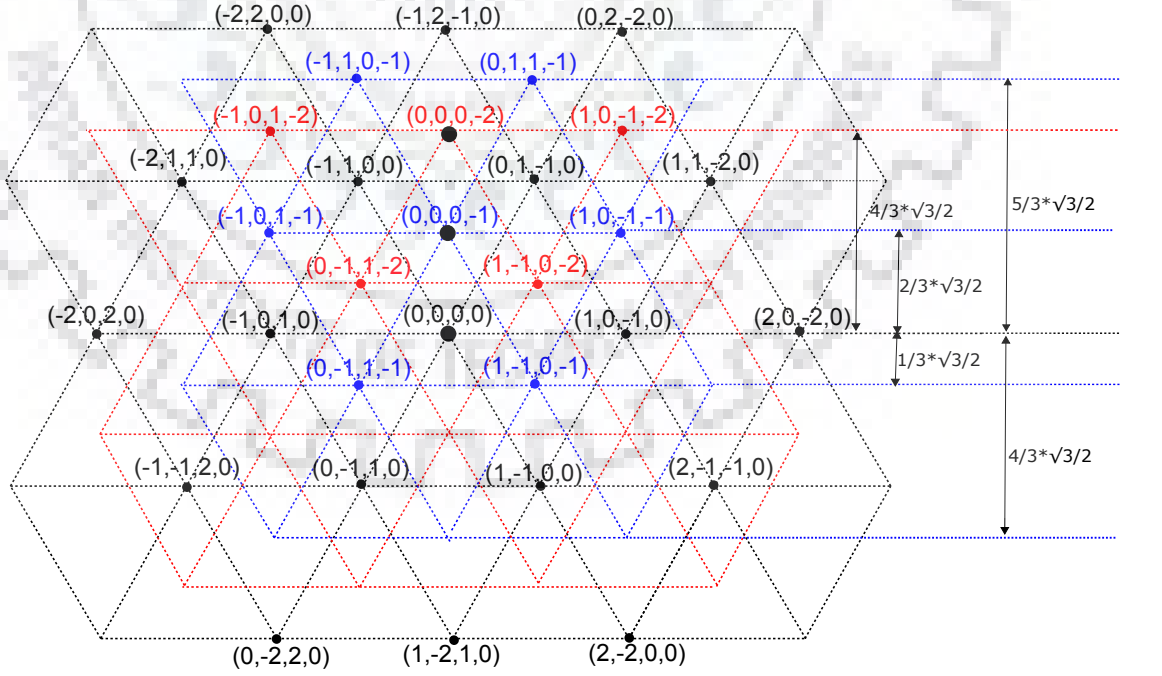

Figure 4.3: Four coordinates system representation of layers below the reference plane. Layer 0, -1, -2 coordinates are represented by black, blue, red color respectively.

Similarly layer 3 sphere which is represent by green colored circle which is filled by light gray have coordinate value $(0,\ 0,\ 0,\ 3)$. For a layer l we have coordinate value as $(0,\ 0,\ 0,\ l)$. An important observation is that all origin of all layers lies on one of the sides of a bigger regular tetrahedron which has one of its faces on the reference plane. Similarly, spheres below the reference plane are represented. One of the difference in representation of layers below the reference plane is that we can only put sphere at position $4-6$ with position 6 is chosen as origin for layer -1 with respect to the layer 0 whose coordinate value is given by $(0,\ 0,\ 0,\ -1)$. Origins of lower layers also lie on the side of a bigger tetrahedron if we shift the face that lies on the reference plane to that layer with one of the vertexes of that face coincides with $(0,\ 0,\ 0,\ -l)$ where l is the layer below the reference plane. Another observation is layer 0 and layer 3 sphere have the same orientation in a sense that their top view coincides as shown in Figure 4.1. We can now say that layer j and layer $j \pm 3$ have the same orientation. All other voxel coordinates at a particular layer can be inductively found by using three coordinates representation with respect to the origin of that layer with the addition of the fourth coordinate as shown in the Figure 4.2 and Figure 4.3.

A spherical voxel has twelve direct neighbors out of which six are on the same layer. Three neighbors are above the layer and three below the layer. For a given voxel coordinate $(x,\ y,\ z,\ w)$ we can determine its direct neighbors.

- Six direct neighbors on same layer are $(x+1,\ y,\ z-1,\ w)$, $(x-1,\ y,\ z+1,\ w)$, $(x-1,\ y+1,\ z,\ w)$, $(x,\ y+1,\ z-1,\ w)$, $(x,\ y-1,\ z+1,\ w)$ and $(x+1,\ y-1,\ z,\ w)$.
- Three direct neighbors on layer above $(x,\ y,\ z,\ w+1)$, $(x-1,\ y+1,\ z,\ w+1)$, $(x,\ y+1,\ z-1,\ w+1)$
- Three direct neighbors on layer below $(x,\ y,\ z,\ w-1)$, $(x,\ y-1,\ z+1,\ w-1)$, $(x+1,\ y-1,\ z,\ w-1)$

4.1 Euclidean Distance between Spherical Voxels

Lets consider the diameter of spherical voxels as one unit. Distance between two adjacent grid points is also one unit.

$$\text{side of tetrahedron} = 1 \text{ unit.}$$

Distance between two points $(x_1,\ y_1,\ z_1)$ and $(x_2,\ y_2,\ z_2)$ in Euclidean three coordinate system is

$$\sqrt{dx^2+dy^2+dz^2}. \tag{4.1}$$

where $dx = x_2 - x_1$, $dy = y_2 - y_1$, $dz = z_2 - z_1$. We need to establish a relationship between the Euclidean distance between two points in four-coordinate. As we have shown the top view of the tetrahedral grid is the triangular grid.

$$\begin{aligned} \therefore \text{ side of triangle} &= 1 \text{ unit.} \\ \text{height of triangle} &= \frac{\sqrt{3}}{2} \text{ unit.} \end{aligned}$$

The difference between the height of two adjacent layers is equal to the height of tetrahedron.

$$\begin{aligned} \text{height of tetrahedron} &= \sqrt{\frac{2}{3}} * \text{side of tetrahedron.} \\ \therefore \text{height of tetrahedron} &= \sqrt{\frac{2}{3}} * 1 = \sqrt{\frac{2}{3}} \text{ unit.} \end{aligned}$$

Let's consider the two points in our four coordinates system as $(x_1,\ y_1,\ z_1,\ w_1)$ and $(x_2,\ y_2,\ z_2,\ w_2)$. We define parameter a, b, c, d as difference between x, y, z, w coordinate respectively.

$$a = x_2 - x_1,\ b = y_2 - y_1,\ c = z_2 - z_1,\ d = w_2 - w_1.$$

The relation that we can establish by careful observation of the tetrahedral grid. Note that our coordinate axes are different from the axes in Euclidean space. It can be verified that x-axis distance between two points always satisfies the following relation. When we move from one point to another along x-axis or parallel to the x-axis in the same layer the y-coordinate remains same. x- coordinate increment by one along positive x-axis direction at the same time z-coordinate decrement by one. In opposite direction z increments by one and x decrement by one.

$$dx = \frac{a-c}{2} \tag{4.2}$$

Euclidean z-axis distance between two points.

$$dz = \sqrt{\frac{2}{3}} * d \tag{4.3}$$

Now we need to determine the relation for dy.The distance dy for $(0,\ 0,\ 0,\ 1)$ and $(0,\ 0,\ 0,\ 2)$ from $(0,\ 0,\ 0,\ 0)$ are $\frac{-2}{3} * \frac{\sqrt{3}}{2}$ and $\frac{-4}{3} * \frac{\sqrt{3}}{2}$ respectively as shown in Figure 4.2. Similarly dy for $(0,\ 0,\ 0,\ -1)$ and $(0,\ 0,\ 0,\ -2)$ are $\frac{2}{3} * \frac{\sqrt{3}}{2}$ and $\frac{4}{3} * \frac{\sqrt{3}}{2}$ respectively as shown in Figure 4.3.

$$\text{For } (0,\ 0,\ 0,\ w_n) \quad dy = \frac{-2w_n}{3} * \frac{\sqrt{3}}{2}$$

The dy between 2 points $(x_1,\ y_1,\ z_1,\ w_n)$ and $(x_2,\ y_2,\ z_2,\ w_n)$ on same layers is $\frac{\sqrt{3}}{2} * b$ where $b = y_2 - y_1$. The origin of other layers is shifted by $\frac{2}{3} * d * \frac{\sqrt{3}}{2}$ from the origin of reference plane ($w = 0$ is consider as reference plane) and other points on that layer have distance from their origin as $b * \frac{\sqrt{3}}{2}$ resulting in total $(b * \frac{\sqrt{3}}{2} - \frac{2}{3} * d * \frac{\sqrt{3}}{2})$ shift and it can be verified from Figure 4.2 and Figure 4.3.

$$\begin{aligned} dy &= \left(b * \frac{\sqrt{3}}{2} - \frac{2}{3} * d * \frac{\sqrt{3}}{2} \right). \qquad (4.4) \\ |dy| &= \left| b * \frac{\sqrt{3}}{2} - \frac{2}{3} * d * \frac{\sqrt{3}}{2} \right|. \\ |dy| &= \frac{\sqrt{3}}{2} * \left| b - \frac{2}{3} * d \right|. \\ |dy| &= \frac{\sqrt{3}}{2} * \left| \frac{3*b - 2*d}{3} \right|. \\ \therefore dy^2 &= \frac{3}{4} * \frac{(3*b - 2*d)^2}{9}. \end{aligned}$$

$$dy^2 = \frac{(3*b-2*d)^2}{12}. \tag{4.5}$$

$$D[(x_1,\, y_1,\, z_1,\, w_1),\, (x_2,\, y_2,\, z_2,\, w_2)] = \sqrt{dx^2+dy^2+dz^2}. \tag{4.6}$$

where D is the Euclidean distance between two points $(x_1,\, y_1,\, z_1,\, w_1)$ and $(x_2,\, y_2,\, z_2,\, w_2)$ First we need to determine value of parameter a, b, c, d as follows.

$$a = x_2 - x_1,\, b = y_2 - y_1,\, c = z_2 - z_1,\, d = w_2 - w_1. \tag{4.7}$$

Using value of Equation 4.2, Equation 4.3, Equation 4.5 in Equation 4.6.

$$\begin{aligned}
D &= \sqrt{\left(\frac{a-c}{2}\right)^2 + \frac{(3*b-2*d)^2}{12} + \left(\sqrt{\frac{2}{3}}*d\right)^2}. \\
D &= \sqrt{\frac{(a^2+c^2-2*a*c)}{2} + \frac{(9*b^2+4*d^2-12*b*d)}{12} + \frac{2*d^2}{3}}. \\
D &= \sqrt{\frac{a^2}{4} + \frac{c^2}{4} - \frac{ac}{2} + \frac{3b^2}{4} + \frac{d^2}{3} - b*d + \frac{2*d^2}{3}}.
\end{aligned}$$

$$D = \sqrt{\frac{a^2}{4} + \frac{c^2}{4} + d^2 + \frac{3b^2}{4} - \frac{ac}{2} - b*d}. \tag{4.8}$$

We have introduced 3 coordinate system in Section 2.1 in such a way that the sum of all three coordinates is always zero for a given point. That relation still holds for 4 coordinate system and can be verified.

$$x_1+y_1+z_1 = 0 \qquad x_2+y_2+z_2 = 0.$$
$$(x_2+y_2+z_2) - (x_1+y_1+z_1) = 0.$$
$$(x_2-x_1) + (y_2-y_1) + (z_2-z_1) = 0.$$

From Equation 4.7

$$a+b+c = 0.$$
$$b = -a-c. \tag{4.9}$$

Put value of b from Equation 4.9 in Equation 4.8.

$$\begin{aligned}
D &= \sqrt{\frac{a^2}{4} + \frac{c^2}{4} + d^2 + \frac{3(-a-c)^2}{4} - \frac{ac}{2} - [(-a-c)*d]}. \\
D &= \sqrt{\frac{a^2}{4} + \frac{c^2}{4} + d^2 + \frac{3(a+c)^2}{4} - \frac{ac}{2} + (a+c)*d}. \\
D &= \sqrt{\frac{a^2}{4} + \frac{c^2}{4} + d^2 + \frac{3(a^2+c^2+2ac)}{4} - \frac{ac}{2} + (a+c)*d}. \\
D &= \sqrt{\frac{a^2}{4} + \frac{c^2}{4} + d^2 + \frac{3a^2}{4} + \frac{3c^2}{4} + \frac{3ac}{2} - \frac{ac}{2} + (a+c)*d}.
\end{aligned}$$

$$D = \sqrt{a^2+c^2+d^2+ac+(a+c)*d}. \tag{4.10}$$

$$D = \sqrt{(x_2-x_1)^2+(z_2-z_1)^2+(w_2-w_1)^2+(x_2-x_1)(z_2-z_1)+(x_2-x_1+z_2-z_1)(w_2-w_1)}. \tag{4.11}$$

When two points belong to same layer i.e. $w_1 = w_2$, $d = 0$.

$$D = \sqrt{a^2+c^2+ac}. \tag{4.12}$$

$$D = \sqrt{(x_2-x_1)^2+(z_2-z_1)^2+(x_2-x_1)(z_2-z_1)}. \tag{4.13}$$

It can be verified that square of D is always an integer. We will use D^2 to compare distances so that floating point operation can be avoided altogether.

4.2 Conversion from Proposed Coordinate System to Cartesian

A point $(x,\ y,\ z)$ in three coordinate system can be represented as Cartesian coordinate $(x_c,\ y_c)$ by the following relation.
$(x,\ y,\ z) \rightarrow (x_c,\ y_c)$ where $x_c = \frac{x-z}{2}$ and $y_c = \sqrt{\frac{3}{2}}y$.

Similarly, four coordinate system can be represented as a 3D point by the following relation.

$(x,\ y,\ z,\ w) \rightarrow (x_c,\ y_c,\ z_c)$ where $x_c = \frac{x-z}{2}$, $y_c = \left(\frac{\sqrt{3}}{2}y - \frac{2}{3} * w * \frac{\sqrt{3}}{2}\right)$, and $z_c = \sqrt{\frac{2}{3}}w$.

5 Geometric Objects on Tetrahedral Grid

In this section, we will represent geometric objects on the tetrahedral grid.

5.1 Layering the Sphere

Spheres can be seen as two identical hemispheres joined together. We can layer hemisphere one layer at a time. The base of hemisphere forms a circular disk. So our first step in layering a sphere is to layer that circle so that other layers can be layered on top of that.

Layering the Circle

Consider the diameter of spherical voxels as one unit and a sphere of radius r units centered at origin $(0,\ 0,\ 0,\ ,0)$.

$$\text{Radius of circle} = r.$$

We can drop w-coordinate in our calculation as it is always same for a layer. Recall from Section 3.3 that a circle has 12 symmetry. We only need to find the voxel coordinates in one of the *duo-decant* (symmetrical half of a sextant). The voxels at sextant axis can be easily plotted by plotting all symmetric voxel of $(r,\ 0,\ -r)$. There are two possibilities of next voxels from current position $q_c(x,\ y,\ z)$ namely $q_1(x-1,\ y+1,\ z)$ and $q_2(x,\ y+1,\ z-1)$. We will computed their distance from the $(0,\ 0,\ 0)$ by using Equation 4.11.

$$D^2(q_1) = (x-1)^2 + z^2 + (x-1)*z.$$
$$D^2(q_2) = x^2 + (z-1)^2 + x*(z-1).$$

It is evident from the Figure 5.1 $D^2(q_1) < r^2$ and $D^2(q_2) > r^2$

$$r^2 - D^2(q_1) > 0 \quad and \quad r^2 - D^2(q_2) < 0.$$

Our decision parameter $p = r^2 - D^2(q_1) + r^2 - D^2(q_2)$ compare the difference of the square of distances. If it is less than zero then q_1 is next voxel otherwise q_2 is next voxel.

$$\begin{aligned} p &= 2r^2 - [D^2(q_1) + D^2(q_2)]. \\ p &= 2r^2 - [(x-1)^2 + z^2 + (x-1)*z + x^2 + (z-1)^2 + x*(z-1)]. \\ p &= 2r^2 - (x^2 - 2x + 1 + z^2 + xz - z + x^2 + z^2 - 2z + 1 + xz - x). \\ p &= 2r^2 - (2x^2 + 2z^2 + 2xz - 3x - 3z + 2). \end{aligned}$$

$$p = 2r^2 - 2x^2 - 2z^2 - 2xz + 3x + 3z - 2. \tag{5.1}$$

Initial value of p at $(r,\ 0,\ -r,\ w)$

$$\begin{aligned} p &= 2r^2 - (2r^2 + 2(-r)^2 + 2r(-r) - 3r - 3(-r) + 2). \\ p &= 2r^2 - (2r^2 + 2r^2 - 2r^2 - 3r + 3r + 2). \\ p &= 2r^2 - 2r^2 - 2. \\ p &= -2. \end{aligned}$$

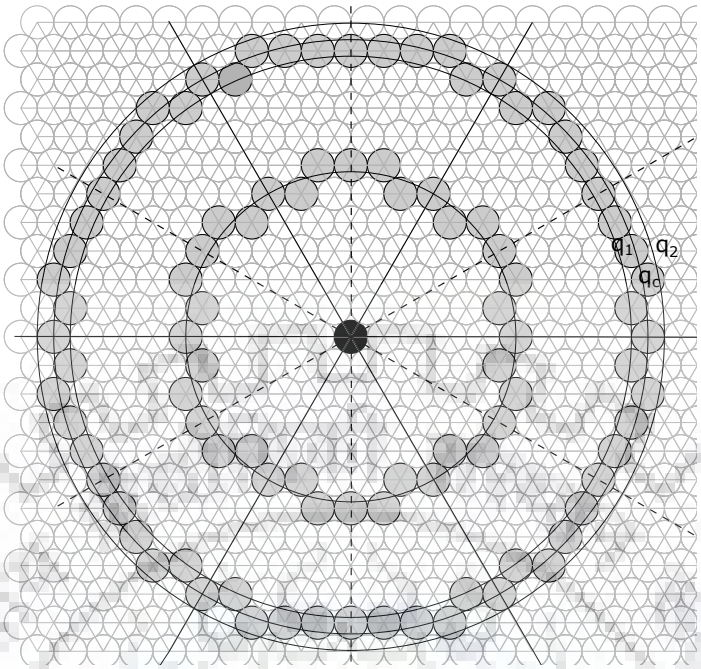

Figure 5.1: Plotting base of a hemisphere.

Value of p at current voxel

$$p_{current} = 2r^2 - 2x^2 - 2z^2 - 2xz + 3x + 3z - 2.$$

Value of p at $(x-1,\ y+1,\ z,\ w)$

$$\begin{aligned} p &= 2r^2 - (2(x-1)^2 + 2z^2 + 2(x-1)z - 3(x-1) - 3z + 2). \\ p &= 2r^2 - (2(x^2 - 2x + 1) + 2z^2 + 2xz - 2z - 3x + 3 - 3z + 2). \\ p &= 2r^2 - 2x^2 + 4x - 2 - 2z^2 - 2xz + 2z + 3x - 3 + 3z - 2. \\ p &= (2r^2 - 2x^2 - 2z^2 - 2xz + 3x + 3z - 2) + 4x - 2 + 2z - 3. \\ p_{next} &= p_{current} + 4x + 2z - 5. \end{aligned}$$

Similarly Value of p at $(x,\ y+1,\ z-1,\ w)$

$$\begin{aligned} p &= 2r^2 - (2x^2 + 2(z-1)^2 + 2x(z-1) - 3x - 3(z-1) + 2). \\ p &= 2r^2 - (2x^2 + 2(z^2 - 2z + 1) + 2xz - 2x - 3x - 3z + 3 + 2). \\ p &= 2r^2 - 2x^2 - 2z^2 + 4z - 2 - 2xz + 2x + 3x + 3z - 3 - 2). \\ p &= (2r^2 - 2x^2 - 2z^2 - 2xz + 3x + 3z - 2) + 4z - 2 + 2x - 3. \\ p_{next} &= p_{current} + 2x + 4z - 5. \end{aligned}$$

A circle of radius r centered at $(x_r,\ y_r,\ z_r)$ can be represent by the following equation.

$$(r - \frac{1}{2})^2 \leq (x - x_r)^2 + (z - z_r)^2 + (x - x_r)(z - z_r) \leq (r + \frac{1}{2})^2.$$

$$r^2 - r + \frac{1}{4} \leq (x - x_r)^2 + (z - z_r)^2 + (x - x_r)(z - z_r) \leq r^2 + r + \frac{1}{4}.$$

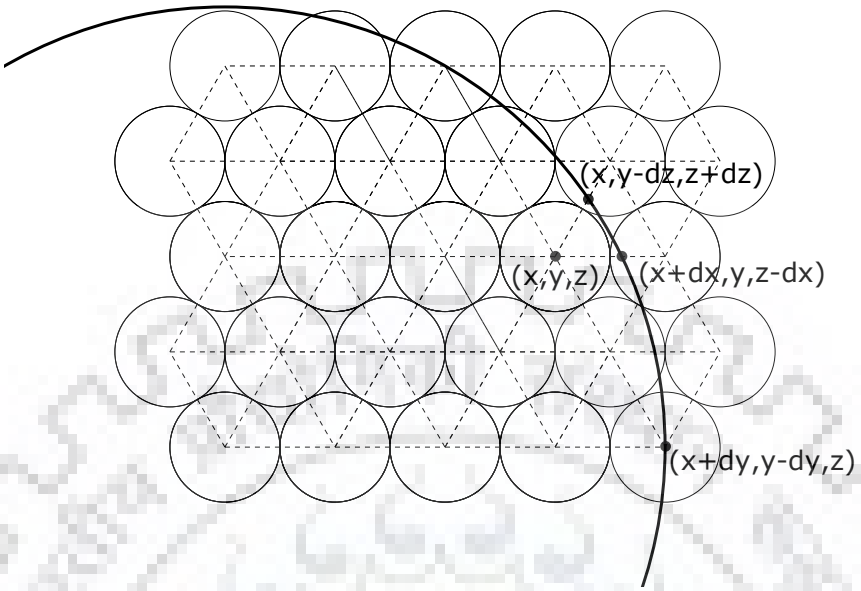

Figure 5.2: Parallel axis distance of a point $(x,\ y,\ z)$ from a circle of radius r.

It is clearly evident from Equation 4.10 and 4.11 that square of distance is always integer. We can drop $\frac{1}{4}$ from both side in our calculation as it does not effect the inequality of equation.

$$r^2 - r < (x-x_r)^2 + (z-z_r)^2 + (x-x_r)(z-z_r) \leq r^2 + r. \tag{5.2}$$

If it is centered at origin $(0,\ 0,\ 0)$

$$r^2 - r < x^2 + z^2 + xz \leq r^2 + r. \tag{5.3}$$

The Equation of Annular disk of inner radius r_1 and outer radius r_2

$$r_1^2 - r_1 < (x-x_r)^2 + (z-z_r)^2 + (x-x_r)(z-z_r) \leq r_2^2 + r_2. \tag{5.4}$$

if $r_1 = r_2$ then Equation 5.4 is same as Equation 5.2. For a Disk $r_1 = 0$ Equation is

$$0 \leq (x-x_r)^2 + (z-z_r)^2 + (x-x_r)(z-z_r) \leq r^2 + r. \tag{5.5}$$

Theorem 2. Isothetic Distance $D_{\|}(x,y,z,r)$ of a point $(x,\ y,\ z)$ from the circle of radius r is the minimum of axis parallel distance.

Proof. Consider a point $p(x,\ y,\ z)$ and a radius r. let's consider the parallel axis distance between the point and circle are dx, dy, and dz in the direction of x-axis, y-axis, and z-axis respectively. The points on the circle are $(x+dx,\ y,\ z-dx)$, $(x+dy,\ y-dy,\ z)$, and $(x,\ y+dz,\ z-dz)$ in the direction of x-axis, y-axis, and z-axis respectively.

$$(x+dx)^2 + (z-dx)^2 + (x+dx)(z-dx) = r^2.$$

$$(x+dy)^2+z^2+(x+dy)z=r^2.$$
$$x^2+(z-dz)^2+x(z-dz)=r^2.$$

Simplifying these equations will give following equations

$$\begin{aligned} dx^2+(x-z)dx-r^2+(x^2+z^2+xz) &= 0.\\ dy^2+(2x+z)dy-r^2+(x^2+z^2+xz) &= 0.\\ dz^2+(-2z-x)dz-r^2+(x^2+z^2+xz) &= 0. \end{aligned}$$

Positive root of these quadratic equations will give parallel axis distance. if these equations have no real roots then value of dx, dy, and dz is taken as ∞.

$$D_{\parallel}(x,y,z,r)=\min(|dx|,|dy|,|dz|).$$

$$dx = \begin{cases} \infty, & 4r^2-3x^2-3z^2-6xz<0 \\ \min\left(\frac{-(x-z)+\sqrt{4r^2-3x^2-3z^2-6xz}}{2}, \frac{-(x-z)-\sqrt{4r^2-3x^2-3z^2-6xz}}{2}\right), & \text{otherwise.} \end{cases}$$

$$dy = \begin{cases} \infty, & 4r^2-3z^2<0 \\ \min\left(\frac{-(2x+z)+\sqrt{4r^2-3z^2}}{2}, \frac{-(2x+z)-\sqrt{4r^2-3z^2}}{2}\right), & \text{otherwise.} \end{cases}$$

$$dz = \begin{cases} \infty, & 4r^2-3x^2<0 \\ \min\left(\frac{(2z+x)+\sqrt{4r^2-3x^2}}{2}, \frac{(2z+x)-\sqrt{4r^2-3x^2}}{2}\right), & \text{otherwise.} \end{cases}$$

$D_{\parallel}$	Duo-decant	value
dx	1 12	$\frac{-(x-z)+\sqrt{4r^2-3x^2-3z^2-6xz}}{2}$
	6 7	$\frac{-(x-z)-\sqrt{4r^2-3x^2-3z^2-6xz}}{2}$
dy	4 5	$\frac{-(2x+z)+\sqrt{4r^2-3z^2}}{2}$
	10 11	$\frac{-(2x+z)-\sqrt{4r^2-3z^2}}{2}$
dx	2 3	$\frac{(2z+x)+\sqrt{4r^2-3x^2}}{2}$
	8 9	$\frac{(2z+x)-\sqrt{4r^2-3x^2}}{2}$

□

Definition 5.1. Naive Circle Set of all point $(x,\ y,\ z)$ for a given radius r which satisfy following conditions

$$r^2 - r < x^2 + z^2 + xz \leq r^2 + r$$

and

Duo-decant	condition
1 12 6 7	$4r^2 - 4x^2 - 4z^2 - 4xz - 2x + 2z - 1 < 0$
4 5 10 11	$4r^2 - 4x^2 - 4z^2 - 4xz - 4x - 2z - 1 < 0$
2 3 8 9	$4r^2 - 4x^2 - 4z^2 - 4xz + 2x + 4z - 1 < 0$

Theorem 3. $D_{\|}(x,y,z,r) = \min(|dx|,|dy|,|dz|) \neq \frac{1}{2}$

Proof. Proof by contradiction
Lets assume $dx = \frac{-(x-z) \pm \sqrt{4r^2-3x^2-3z^2-6xz}}{2} = \pm\frac{1}{2}$

$$-(x-z) \pm \sqrt{4r^2 - 3x^2 - 3z^2 - 6xz} = \pm 1.$$

$$\pm\sqrt{4r^2 - 3x^2 - 3z^2 - 6xz} = \pm 1 + (x-z).$$

After squaring and simplifying both sides

$$4r^2 - 4x^2 - 4z^2 - 4xz - 2x + 2z = 1.$$

$$2(2r^2 - 2x^2 - 2z^2 - 2xz \mp x \pm z) = 1.$$

Since r, x, and z are integers. LHS is always even and RHS is odd, which contradicts our assumption.

$$4r^2 - 4x^2 - 4z^2 - 4xz \mp 2x \pm 2z \neq 1.$$

Similarly we will proof for dy and dz

$$2(2r^2 - 2x^2 - 2z^2 - 2xz - 2x - z) \neq 1.$$

$$2(2r^2 - 2x^2 - 2z^2 - 2xz + x + 2z) \neq 1.$$

□

Theorem 4. if $para = 0$ at $(x,\ y,\ z)$, then isothetic distance of rightmost voxel $(x,\ y+1,\ z-1)$ is always less than $\frac{1}{2}$.

$$D_{\|}(x,\ y+1,\ z-1) < \frac{1}{2}.$$

Proof. Since the center of voxel $(x,\ y+1,\ z-1)$ lies outside the circle, it will satisfy the following inequality.

$$D^2 = x^2 + (z-1)^2 + x(z-1) > r^2.$$

If the isothetic distance of $(x,\ y+1,\ z-1)$ is less than $\frac{1}{2}$ then it will satisfy the following equation

$$D_{\|}(x,\ y,\ z) < \frac{1}{2} \qquad \text{if } 4r^2 - 4x^2 - 4z^2 - 4xz - 2x + 2z - 1 < 0 \tag{5.6}$$

$$D_{\|}(x,\ y,\ z) > \frac{1}{2} \qquad \text{if } 4r^2 - 4x^2 - 4z^2 - 4xz - 2x + 2z - 1 > 0.$$

$$para = 2r^2 - 2x^2 - 2z^2 - 2xz + 3x + 3z - 2 = 0.$$

$$4r^2 - 4x^2 - 4z^2 - 4xz = -6x - 6z + 4 \tag{5.7}$$

Checking isothetic condition for $(x,\ y+1,\ z-1)$

$$\begin{aligned} 4r^2 - 4x^2 - 4(z-1)^2 - 4x(z-1) - 2x + 2(z-1) - 1 &< 0. \\ 4r^2 - 4x^2 - 4z^2 - 4xz + 2x - 6z - 7 &< 0. \end{aligned}$$

using Equation 5.7

$$\begin{aligned} -6x - 6z + 4 + 2x + 10z - 7 &< 0. \\ -4x + 4z - 3 &< 0. \\ -4(x-z) - 3 &< 0. \end{aligned}$$

$(x-z)$ is positive in duo-decant 1 and 12

$$\begin{aligned} -4(x-z) &< 0. \\ -4(x-z) - 3 &< 0. \\ \therefore D_{\|}(x,\ y+1,\ z-1) &< \frac{1}{2}. \end{aligned}$$

Similarly, we can show that isothetic distance of $(x-1,\ y+1,\ z)$ is greater than $\frac{1}{2}$

$$\begin{aligned} 4r^2 - 4x^2 - 4z^2 - 4xz - 2x + 2z - 1 &> 0. \\ 4r^2 - 4(x-1)^2 - 4z^2 - 4(x-1)z - 2(x-1) + 2z - 1 &> 0. \\ 4r^2 - 4x^2 - 4z^2 - 4xz + 6x + 6z - 3 &> 0. \end{aligned}$$

Using Equation 5.7

$$\begin{aligned} -6x - 6z + 4 + 6x + 6z - 3 &> 0. \\ 1 &> 0. \\ D_{\|}(x-1,\ y+1,\ z) &> \frac{1}{2}. \end{aligned}$$

In case of tie ($para = 0$), we will always select the rightmost voxel.

□

The Algorithm to layer the base of the hemisphere is summarized as follows.

Algorithm 1 Circle Layering

1: **procedure** CIRCLE(x_r, y_r, z_r, w_r, r) ▷ Circle of radius r centered at (x_r, y_r, z_r, w_r)
2: $x \leftarrow r + x_r \quad y \leftarrow y_r \quad z \leftarrow -r + z_r$
3: plot12(x, y, z, w_r) ▷ Plot voxel on the sextant axes
4: $p \leftarrow -2$
5: **while** $x - 1 > y$ **do**
6: **if** $p < 0$ **then**
7: PLOT12($x-1$, $y+1$, z, w_r)
8: $p \leftarrow p + (x << 2) + (z << 1) - 5$ ▷ $p = p + 4x + 2z - 5$
9: $x \leftarrow x - 1$
10: **else**
11: PLOT12(x, $y+1$, $z-1$, w_r)
12: $p \leftarrow p + (x << 1) + (z << 2) - 5$ ▷ $p = p + 2x + 4z - 5$
13: $z \leftarrow z - 1$
14: $y \leftarrow y + 1$
15: **return** All plotted voxels ▷ All plotted voxels and their symmetric points
16: **end procedure**

17: **procedure** PLOT12(x, y, z, w)
18: PLOT(x, y, z, w)
19: PLOT(y, x, z, w)
20: PLOT($-y$, $-z$, $-x$, w)
21: PLOT($-x$, $-z$, $-y$, w)
22: PLOT(z, x, y, w)
23: PLOT(z, y, x, w)
24: PLOT($-x$, $-y$, $-z$, w)
25: PLOT($-y$, $-x$, $-z$, w)
26: PLOT(y, z, x, w)
27: PLOT(x, z, y, w)
28: PLOT($-z$, $-x$, $-y$, w)
29: PLOT($-z$, $-y$, $-x$, w)
30: **end procedure**

31: **procedure** PLOT(x, y, z, w)
32: plot voxel (x, y, z, w)
33: **end procedure**

The loop in line 5 terminates just before the voxel that is on the duo-decant boundary. For even value of r voxel on the duo-decant boundary have $x = y$ and for odd value of r it have $x - 1 = y$. These boundary voxels can be next possible voxel from current voxel which is just before the boundary voxel. Experimental results shows that loop runs exactly $\lceil \frac{r}{2} \rceil + \lceil \frac{r}{12} \rceil$ times. Circles plotted by Algorithm 1 for $r = 15$ and $r = 16$ are shown in 5.3.

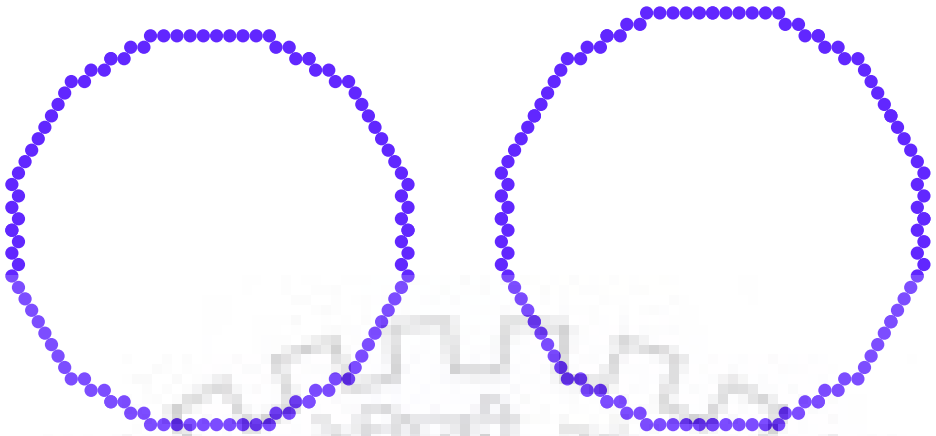

(a) Circle of $r = 15$ (b) Circle of $r = 16$

Figure 5.3: Circle plotted for $r = 15$ and $r = 16$ by Algorithm 1

Theorem 5. Naive circle is minimal and connected.

Proof. The algorithm uses 12 symmetry. In duo-decant 1 for a given value of y, we are selecting only one voxel from next possible voxels. This way minimality occurs in duo-decant 1. The 12 symmetry ensures the minimality in other duo-decant, thus making the circle minimal.

It is not harder to see that voxels inside a duo-decant are connected as we are moving to direct neighbors from each voxel. We need to show that the voxels at duo-decant boundaries will form a connected set. The last voxel in a duo-decant has this property.

$$x = y \text{ For even value of } |z|.$$

$$x - 1 = y \text{ For odd value of } |z|.$$

For a sextant, the last voxel of two duo-decant will be connected. for the even value of r voxel where $x == y$ will be at the duo-decant boundary. Thus making voxel inside a sextant connected. similarly, we can show that same argument is valid for other sextant duo-decant. For odd value of r the last voxels have $x - 1 = y$ in one duo-decant and $x = y - 1$ in other duo-decant. It is clear that these two voxels are connected. These are direct neighbors of each other.

Now we need to show that the voxel at sextant boundary will be connected. The last voxel in sextant-I have coordinate $(0,\ r,\ -r)$. Since the Initial value of *para* is -2, the voxel $(1,\ r,\ -r-1)$ will be the first voxel in sextant-II. As we can see these two voxel are direct neighbors of each other. Similar argument can be used for other sextant boundary.

□

Theorem 6. Separability $D(d_1, d_2) \geq \sqrt{3}$

Proof. The voxels inside the circle must satisfy the following equation for a given value of r

$$D_1{}^2 \leq r^2 - r.$$

Similarly voxels outside the circle must satisfy the following equation.

$$D_2{}^2 > r^2 + r.$$

where D_1 and D_2 is the square of distance from the origin $(0,\ 0,\ 0)$.

$$D_2{}^2 - D_1{}^2 > 2r.$$

Lets consider a voxel inside the circle as d_1 and voxel outside the circle as d_2. $D(d_1,d_2)$ is the euclidean distance between d_1 and d_2. if voxel $(x,\ y,\ z)$ is part of a circle. d_1 can be $(x-dx1,\ y-dy1,\ z-dz1)$ and d_2 can be $(x-dx2,\ y-dy2,\ z-dz2)$ where $dx1$, $dx2$, $dy1$, $dy2$, $dz1$, $dz2$ are integers.

$$[D(d_1,d_2)]^2 = (dx2-dx1)^2 + (dz2-dz1)^2 + (dx2-dx1)(dz2-dz1).$$

maximum value of $dx2-dx1$ and $dz2-dz1$ can be ∞ minimum value of $dx2-dx1=1$ and $dz2-dz1=-2$ in sextant-I. It can be seen along the boundary between duo-decant 1 and 2.

$$[D(d_1,d_2)]^2 = 1+4-2.$$

$$[D(d_1,d_2)]^2 = 3.$$

$$[D(d_1,d_2)] \geq \sqrt{3}.$$

□

Layering the Disk

Disk boundary is layered by Algorithm 1. The inner voxels of the disk can be layered. The Equation of the Disk is given by Equation 5.5

$$0 < (x-x_r)^2 + (z-z_r)^2 + (x-x_r)(z-z_r) \leq r^2 + r \tag{5.8}$$

Running Algorithm 1 $r+1$ times from radius 0 to r will not given complete disk. Some voxels may be missing as the circle layering does not satisfy the tiling property as shown in Figure 5.4.

Another approach that uses hexagon can be used for layering the disk. We only need to find hexagon voxels in one duo-decant. The disk boundary is circumcircle of a hexagon H_1 of side h_1, It is also incircle of hexagon H_2 of side h_2 as shown in Figure 5.5.

$$h_1 < h_2, \quad h_1 = r, \quad h_2 = \frac{2r}{\sqrt{3}}.$$

Similarly for a annular disk of inner radius r_1 and outer radius r_2 following relation holds

$$h_1 < h_2 < h_3, \quad h_1 = r_1, \quad h_2 = r_2, \quad h_3 = \frac{2r_2}{\sqrt{3}}.$$

It is obvious that all voxels inside H_1 satisfy Equation 5.8. To layer remaining voxels of the disk, we need to make sure voxels that are inside H_2 which are not part of H_1 must satisfy Equation 5.8.

The Algorithm to layer the Disk can be summarized as follows. Voxels inside H_1 can be found

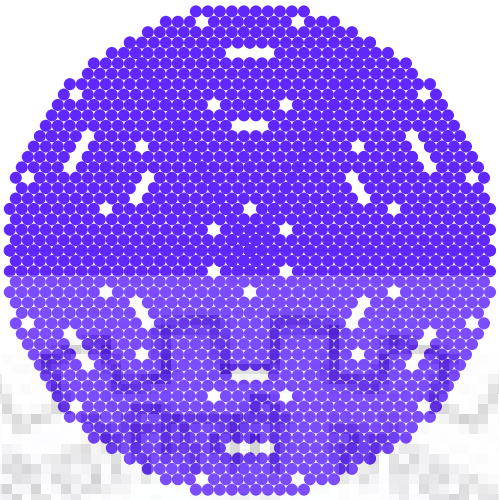

Figure 5.4: Layering circle from radius 0 to 20 results in missing voxels which shows that tiling property does not hold.

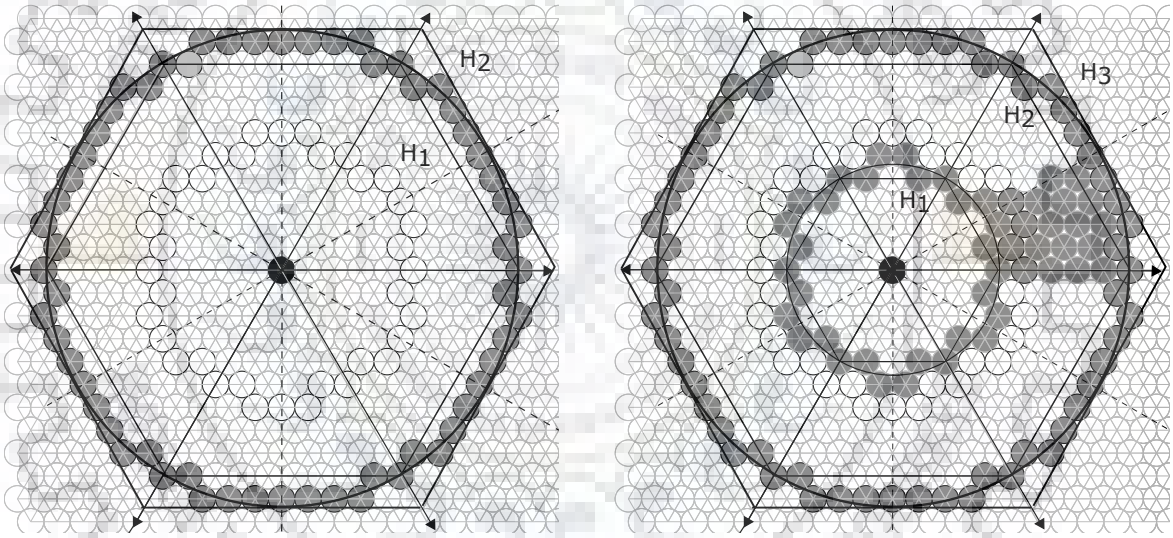

(a) Disk (b) Annular Disk

Figure 5.5: Incircle and circumcircle of Hexagons in Disk and Annular Disk

out by line 3-7. Voxels that are inside H_2 that are not part of H_1 can be found out by line 8-13. Line 11 ensures that voxels satisfy Equation 5.8.

Algorithm 2 Disk_layering

procedure DISK(x_r, y_r, z_r, w_r, r) ▷ Disk of radius r centered at (x_r, y_r, z_r, w_r)
  $x \leftarrow r + x_r \quad y \leftarrow y_r \quad z \leftarrow -r + z_r \quad w \leftarrow w_r$
  for $i = 0; i \leq r; i++$ **do**
    $x \leftarrow i + x_r \quad z \leftarrow -i + z_r \quad y \leftarrow y_r$
    for $j = 0; j < \lfloor \frac{i+2}{2} \rfloor; j++$ **do**
      PLOT12(x, y, z, w) ▷ Procedure PLOT12 of Algorithm 1
      $x \leftarrow x - 1 \quad y \leftarrow y + 1$
  for $i = r + 1; i \leq r + \lfloor \frac{r}{6} \rfloor; i++$ **do**
    $x \leftarrow i + x_r \quad z \leftarrow -i + z_r \quad y \leftarrow y_r$
    for $j = 0; j < \lfloor \frac{i+2}{2} \rfloor; j++$ **do**
      if $r^2 + r \geq x^2 + z^2 + xz$ **then** ▷ Equation 5.8
        PLOT12(x, y, z, w) ▷ Procedure PLOT12 of Algorithm 1
      $x \leftarrow x - 1 \quad y \leftarrow y + 1$
  return All plotted voxels ▷ All plotted voxels and their symmetric points
end procedure

Algorithm 3 Annular_Disk

procedure ANNULAR_DISK(x_r, y_r, z_r, w_r, r_1, r_2)
  $w \leftarrow w_r$
  for $i = r_1; i \leq r_2; i++$ **do**
    $x \leftarrow i + x_r \quad y \leftarrow y_r \quad z \leftarrow -i + z_r$
    for $j = 0; j < \lfloor \frac{i+2}{2} \rfloor; j++$ **do**
      if voxel $V(x, y, z, w)$ satisfy Equation 5.4 **then**
        PLOT12(x, y, z, w) ▷ Procedure PLOT12 of Algorithm 1
      $x \leftarrow x - 1 \quad y \leftarrow y + 1$
  for $i = r_2 + 1; i \leq r_2 + \lfloor \frac{r_2}{6} \rfloor; i++$ **do**
    $x \leftarrow i + x_r \quad y \leftarrow y_r \quad z \leftarrow -i + z_r$
    for $j = 0; j < \lfloor \frac{i+2}{2} \rfloor; j++$ **do**
      if voxel $V(x, y, z, w)$ satisfy Equation 5.4 **then**
        PLOT12(x, y, z, w) ▷ Procedure PLOT12 of Algorithm 1
      $x \leftarrow x - 1 \quad y \leftarrow y + 1$
  return All plotted voxels ▷ All plotted voxels and their symmetric points
end procedure

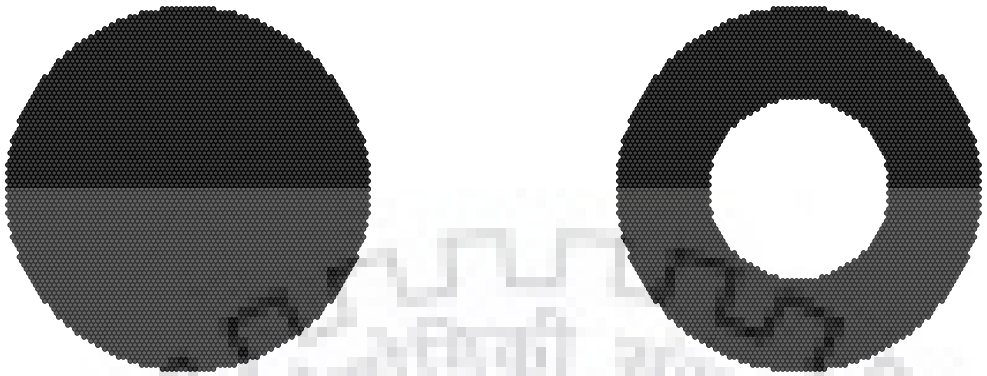

(a) Disk of $r = 40$ (b) Annular disk of $r_1 = 20$ and $r_2 = 40$

Figure 5.6: Disk plotted by Algorithm 2 and 3

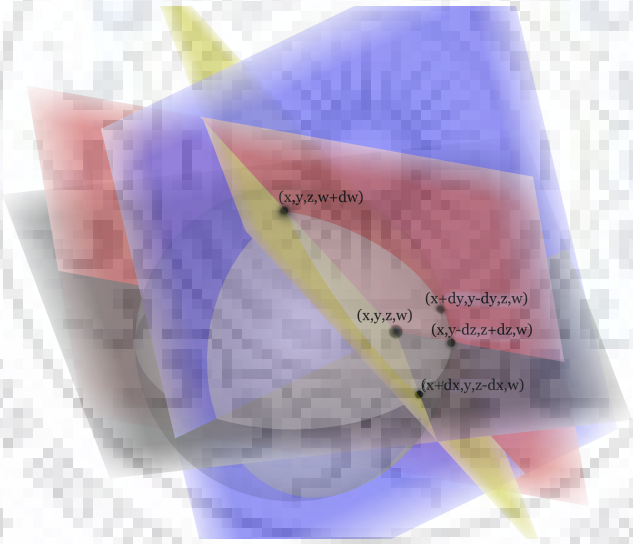

Figure 5.7: Parallel plane distance of a point $(x,\ y,\ z,\ w)$ from a sphere of radius r.

Theorem 7. Isothetic distance $D_{\parallel}(x,y,z,w,r)$ of a point $(x,\ y,\ z,\ w)$ for a sphere of radius r is the minimum parallel plane distance from the sphere.

Proof. Consider a point $p(x,\ y,\ z,\ w)$ and a radius r. lets consider the parallel plane distance between the point and sphere are dx, dy, dz, dw in the direction of x-plane, y-plane, z-plane, w-plane respectively. The points on the sphere are $(x+dx,\ y,\ z-dx,\ w)$, $(x+dy,\ y-dy,\ z,\ w)$, $(x,\ y+dz,\ z-dz,\ w)$, $(x,\ y,\ z,\ w+dw)$ in the direction of x-plane, y-plane, z-plane, w-plane

respectively.

$$\begin{aligned}
(x+dx)^2+(z-dx)^2+(x+dx)(z-dx)+w^2+(x+dx+z-dx)w &= r^2.\\
(x+dy)^2+z^2+(x+dy)z+w^2+(x+dy+z)w &= r^2.\\
x^2+(z-dz)^2+x(z-dz)+w^2+(x+z-dx)w &= r^2.\\
x^2+z^2+xz+(w+dw)^2+(x+z)(w+dw) &= r^2.
\end{aligned}$$

Simplifying these equations will give following equations

$$\begin{aligned}
dx^2+(x-z)dx-r^2+(x^2+z^2+xz+w^2+(x+z)w) &= 0.\\
dy^2+(2x+z+w)dy-r^2+(x^2+z^2+xz+w^2+(x+z)w) &= 0.\\
dz^2+(-2z-x+w)dz-r^2+(x^2+z^2+xz+w^2+(x+z)w) &= 0.\\
dw^2+(x+z+2w)dy-r^2+(x^2+z^2+xz+w^2+(x+z)w) &= 0.
\end{aligned}$$

Positive root of these quadratic equations will give parallel axis distance. if these equations have no real roots then value of dx, dy, dz, dw is taken as ∞.

$$D_{\|}(x,y,z,r) = \min(|dx|,|dy|,|dz|,|dw|).$$

Due to asymmetric nature of w-axis isothetic distance for the sphere is not useful. □

Symmetry in Sphere

A sphere have two points of symmetry in each hemisphere. For a voxel $(x,\ y,\ z,\ w)$ in one hemisphere we have voxel $(-x,\ -y,\ -z,\ -w)$ in other hemisphere. There distance from the origin $(0,\ 0,\ 0,\ 0)$ is same. By using Equation 4.11

$$D = \sqrt{(-x)^2+(-z)^2+(-w)^2+(-x)(-z)+(-x-z)(-w)}.$$

$$D = \sqrt{x^2+z^2+w^2+xz+(x+z)w}.$$

which is equal to the distance of voxel $(x,\ y,\ z,\ w)$ from the origin.

Layering the Hemisphere

A Hemisphere can be Layered one layer at a time. We have already layered 0^{th} layer by Algorithm 2. We will generate 1^{st} layer by using the direct upper layer neighbors of layer 0. Similarly, we will generate 2^{nd} layer by direct upper layer neighbors of layer 1. Recall that layer l and $l+3$ have the same orientation. We can establish a relation between them and layer $l+3$ can be directly found by layer l. Layer 0, 1, and 2 will form a set of three consecutive layers. Similarly layer 3, 4, and 5 will form another set and so on. We need to find how many such sets are there for a hemisphere of radius r. Let L be the number of sets. Euclidean z-axis

Distance between two consecutive layer is $\sqrt{\frac{2}{3}}$ unit.

$$\begin{aligned}
\text{Total number of layers} &= 3L. \\
\text{Height} = (3L-1) * \sqrt{\frac{2}{3}} &= r. \\
(3L-1) * \sqrt{\frac{2}{3}} &= r. \\
(3L-1)^2 * \frac{2}{3} &= r^2. \\
(3L-1)^2 &= \frac{3r^2}{2}. \\
(3L)^2 &> \frac{3r^2}{2}. \\
L^2 &> \frac{r^2}{6}. \\
L &> \sqrt{\frac{r^2}{6}} \quad L \text{ is an integer.} \\
\therefore L &= \left\lceil \sqrt{\frac{r^2}{6}} \right\rceil.
\end{aligned}$$

Consider 0^{th} layer voxel as$(x_0,\ y_0,\ z_0,\ 0)$, 1^{st} layer voxel as $(x_1,\ y_1,\ z_1,\ 1)$, 2^{nd} layer voxel as $(x_2,\ y_2,\ z_2,\ 2)$.

For $i = 1$ to $L-1$

Layer $3i$ voxel $(x_0 - i,\ y_0 + 2i,\ z_0 - i,\ 3i)$ have same orientation as $(x_0,\ y_0,\ z_0,\ 0)$.

Layer $3i+1$ voxel $(x_1 - i,\ y_1 + 2i,\ z_1 - i,\ 3i+1)$ have same orientation as $(x_1,\ y_1,\ z_1,\ 1)$.

Layer $3i+2$ voxel $(x_2 - i,\ y_2 + 2i,\ z_2 - i,\ 3i+2)$ have same orientation as $(x_2,\ y_2,\ z_2,\ 2)$.
Equation 5.2 can be extended to Sphere of radius r centered at $(x_r,\ y_r,\ z_r,\ w_r)$.

$$r^2 - r < (x-x_r)^2 + (z-z_r)^2 + (w-w_r)^2 + (x-x_r)(z-z_r) + (z-z_r+x-x_r)(w-w_r) \leq r^2 + r. \tag{5.9}$$

If center is at origin

$$r^2 - r < x^2 + z^2 + w^2 + xz + (x+z)w \leq r^2 + r. \tag{5.10}$$

If the Sphere is solid

$$0 \leq (x-x_r)^2 + (z-z_r)^2 + (w-w_r)^2 + (x-x_r)(z-z_r) + (z-z_r+x-x_r)(w-w_r) \leq r^2 + r. \tag{5.11}$$

A spherical shell of inner radius r_1 and outer radius r_2 have equation as follows where $r_1 < r_2$

$$r_1^2 - r_1 < (x-x_r)^2 + (z-z_r)^2 + (w-w_r)^2 + (x-x_r)(z-z_r) + (z-z_r+x-x_r)(w-w_r) \leq r_2^2 + r_2. \tag{5.12}$$

Sphere is hollow if $r_1 = r_2$ and sphere is solid if $r_1 = 0$.

Algorithm 4 Hollow_Hemisphere

procedure HOLLOW_HEMISPHERE(x_r, y_r, z_r, w_r, r)
    Layer_0, Layer_1, and Layer_2 be the empty list of voxels
    $L = \left\lceil \sqrt{\frac{r^2}{6}} \right\rceil$
    CIRCLE(x_r, y_r, z_r, w_r, r) ▷ Algorithm 1
    Layer_0 ←DISK(x_r, y_r, z_r, w_r, r) ▷ Algorithm 2
    Layer_1, Layer_2 ← LAYER_1_2(Layer_0)
    for $j = 1$ to $L-1$ **do**
        for Each voxel $(x, y, z, w) \in$ Layer_3(j-1) **do**
            if voxel $(x-j, y+2j, z-j, 3j)$ satisfy Equation 5.11 **then**
                Add voxel $(x-j, y+2j, z+j, 3j)$ to Layer_3j
            if voxel $(x-j, y+2j, z-j, 3j)$ satisfy Equation 5.9 **then**
                plot $(x-j, y+2j, z-j, 3j)$
        for Each voxel $(x, y, z, w) \in$ Layer_3(j-1)+1 **do**
            if voxel $(x-j, y+2j, z-j, 3j+1)$ satisfy Equation 5.11 **then**
                Add voxel $(x-j, y+2j, z-j, 3j+1)$ to Layer_3j+1
            if voxel $(x-j, y+2j, z-j, 3j+1)$ satisfy Equation 5.9 **then**
                plot $(x-j, y+2j, z-j, 3j+1)$
        for Each voxel $(x, y, z, w) \in$ Layer_3(j-1)+2 **do**
            if voxel $(x-j, y+2j, z-j, 3j+2)$ satisfy Equation 5.11 **then**
                Add voxel $(x-j, y+2j, z-j, 3j+2)$ to Layer_3j+2
            if voxel $(x-j, y+2j, z-j, 3j+2)$ satisfy Equation 5.9 **then**
                plot $(x-j, y+2j, z-j, 3j+2)$
end procedure

procedure LAYER_1_2(Layer_0)
    for $i = 0$ to 1 **do**
        for Each voxel $(x, y, z, w) \in$ Layer_i **do**
            if Voxel $U_1(x, y, z, w+1) \notin$ Layer_i+1 and U_1 satisfy Equation 5.11 **then**
                Add voxel $U_1(x, y, z, w+1)$ to Layer_i+1
            if U_1 satisfy Equation 5.9 **then**
                plot $(x, y, z, w+1)$
            if Voxel $U_2(x-1, y+1, z, w+1) \notin$ Layer_i+1 and U_2 satisfy Equation 5.11 **then**
                Add voxel $U_2(x-1, y+1, z, w+1)$ to Layer_i+1
            if U_2 satisfy Equation 5.9 **then**
                plot $(x-1, y+1, z, w+1)$
            if Voxel $U_3(x, y+1, z-1, w+1) \notin$ Layer_i+1 and U_3 satisfy Equation 5.11 **then**
                Add voxel $U_3(x, y+1, z-1, w+1)$ to Layer_i+1
            if U_3 satisfy Equation 5.9 **then**
                plot $(x, y+1, z-1, w+1)$
    return Layer_1, Layer_2
end procedure

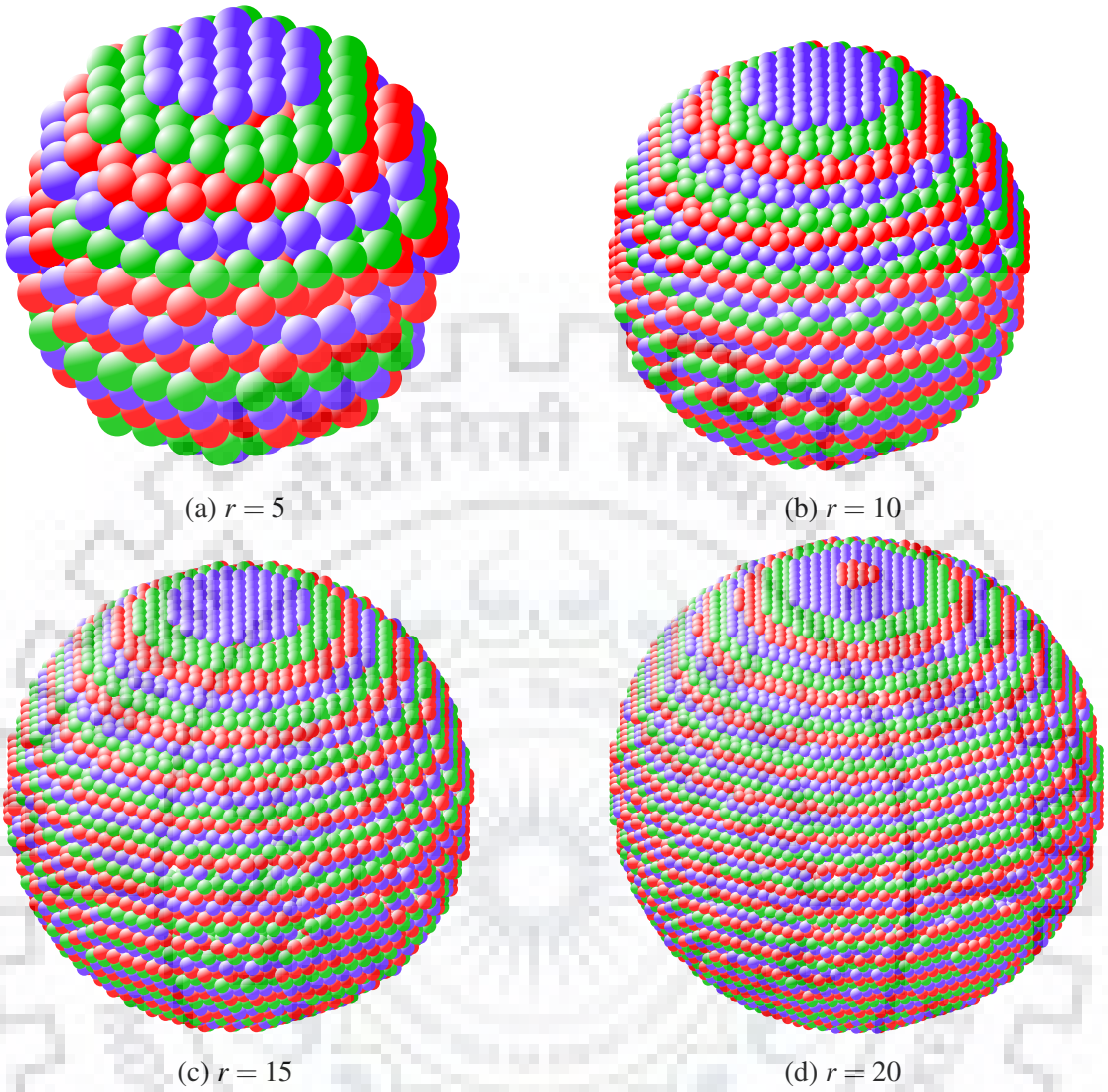

(a) $r = 5$ (b) $r = 10$

(c) $r = 15$ (d) $r = 20$

Figure 5.8: Hollow spheres plotted by Algorithm 4. Using two symmetry of sphere complete sphere is plotted. Layer $3i$ is shown as blue color voxels. similarly, layer $3i+1$ and $3i+2$ are shown as red and green color voxels respectively. According to two symmetry layer, $3i$ and $-3i$ are of same color voxels. Similarly layer $-3(i+1)$ and $-3(i+2)$ are of same color as layer $3(i+1)$ and $3(i+2)$ respectively.

We have generated only one hemisphere by the Algorithm 4. Other hemisphere is plotted by using two symmetry of the sphere. For a voxel $(x,\ y,\ z,\ w)$, two voxel are plotted $(x,\ y,\ z,\ w)$ and $(-x,\ -y,\ -z,\ -w)$. Results are shown in Figure 5.8 for smaller value of r. As the value of r increase the spherical smoothness increases. The color encoding of layers in Figure 5.8 will be used in upcoming sections.

Algorithm 5 Hemispherical_Shell

procedure HEMISPHERICAL_SHELL(x_r, y_r, z_r, w_r, r_1, r_2)
    Layer_0, Layer_1, and Layer_2 be the empty list of voxels
    $L = \left\lceil \sqrt{\frac{r_2^2}{6}} \right\rceil$
    ANNULAR_DISK(x_r, y_r, z_r, w_r, r_1, r_2) ▷ Algorithm 3
    Layer_0 ←DISK(x_r, y_r, z_r, w_r, r_2) ▷ Algorithm 2
    Layer_1, Layer_2 ← SHELL_LAYER_1_2(Layer_0)
    for $j = 1$ to $L-1$ **do**
        for Each voxel $(x, y, z, w) \in$ Layer_3(j-1) **do**
            if voxel $(x-j, y+2j, z-j, 3j)$ satisfy Equation 5.11 **then**
                Add voxel $(x-j, y+2j, z+j, 3j)$ to Layer_3j
            if voxel $(x-j, y+2j, z-j, 3j)$ satisfy Equation 5.12 **then**
                plot $(x-j, y+2j, z-j, 3j)$
        for Each voxel $(x, y, z, w) \in$ Layer_3(j-1)+1 **do**
            if voxel $(x-j, y+2j, z-j, 3j+1)$ satisfy Equation 5.11 **then**
                Add voxel $(x-j, y+2j, z-j, 3j+1)$ to Layer_3j+1
            if voxel $(x-j, y+2j, z-j, 3j+1)$ satisfy Equation 5.12 **then**
                plot $(x-j, y+2j, z-j, 3j+1)$
        for Each voxel $(x, y, z, w) \in$ Layer_3(j-1)+2 **do**
            if voxel $(x-j, y+2j, z-j, 3j+2)$ satisfy Equation 5.11 **then**
                Add voxel $(x-j, y+2j, z-j, 3j+2)$ to Layer_3j+2
            if voxel $(x-j, y+2j, z-j, 3j+2)$ satisfy Equation 5.12 **then**
                plot $(x-j, y+2j, z-j, 3j+2)$
end procedure

procedure SHELL_LAYER_1_2(Layer_0)
    for $i = 0$ to 1 **do**
        for Each voxel $(x, y, z, w) \in$ Layer_i **do**
            if Voxel $U_1(x, y, z, w+1) \notin$ Layer_i+1 and U_1 satisfy Equation 5.11 **then**
                Add voxel $U_1(x, y, z, w+1)$ to Layer_i+1
            if U_1 satisfy Equation 5.12 **then**
                plot $(x, y, z, w+1)$
            if Voxel $U_2(x-1, y+1, z, w+1) \notin$ Layer_i+1 and U_2 satisfy Equation 5.11 **then**
                Add voxel $U_2(x-1, y+1, z, w+1)$ to Layer_i+1
            if U_2 satisfy Equation 5.12 **then**
                plot $(x-1, y+1, z, w+1)$
            if Voxel $U_3(x, y+1, z-1, w+1) \notin$ Layer_i+1 and U_3 satisfy Equation 5.11 **then**
                Add voxel $U_3(x, y+1, z-1, w+1)$ to Layer_i+1
            if U_3 satisfy Equation 5.12 **then**
                plot $(x, y+1, z-1, w+1)$
    return Layer_1, Layer_2
end procedure

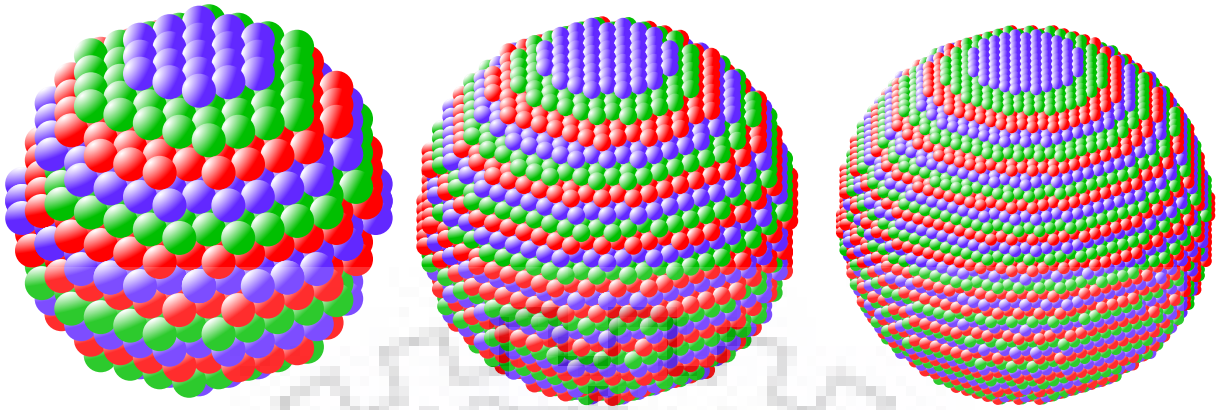

(a) $r = 5$ (b) $r = 10$ (c) $r = 15$

Figure 5.9: Solid spheres plotted by Algorithm 5 using two symmetry of sphere. The color encoding used in Figure 5.8 is used to represent layers. Inner radius is $r_1 = 0$ and outer radius is $r_2 = r$ for solid sphere.

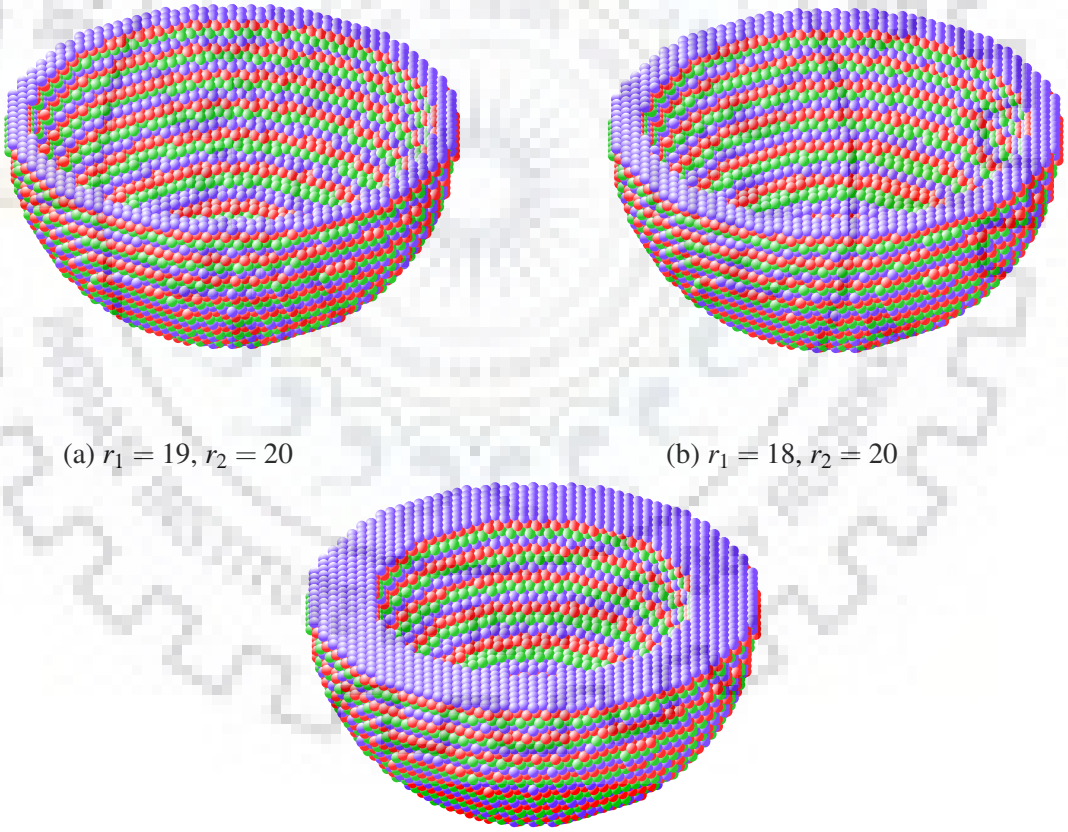

(a) $r_1 = 19$, $r_2 = 20$ (b) $r_1 = 18$, $r_2 = 20$

(c) $r_1 = 15$, $r_2 = 20$

Figure 5.10: Hemispherical shells plotted by Algorithm 5 for $r = 20$ of thickness 1, 2, and 5. If we consider thickness of hollow sphere as zero, Then thickness of spherical shell is $r_2 - r_1$.

5.2 Sphere Printing Algorithm

Consider a point $(x,\ y,\ z,\ w)$. Square of distance from the origin $(0,\ 0,\ 0,\ 0)$ is

$$p_0 = D^2 = x^2 + z^2 + w^2 + xz + (x+z)w$$

for $(0,\ 0,\ 0,\ 0)$ $p_0 = 0$. Direct neighbors of $(x,\ y,\ z,\ w)$ are $(x+1,\ y,\ z-1,\ w)$, $(x,\ y+1,\ z-1,\ w)$, $(x-1,\ y+1,\ z,\ w)$, $(x-1,\ y,\ z+1,\ w)$, $(x,\ y-1,\ z+1,\ w)$ and $(x+1,\ y-1,\ z,\ w)$ in 0°, 60°, 120°, 180°, 240° and 300° direction respectively.

$$\begin{aligned}
p_1 &= (x+1)^2 + (z-1)^2 + w^2 + (x+1)(z-1) + (x+1+z-1)w. \\
p_2 &= x^2 + (z-1)^2 + w^2 + x(z-1) + (x+z-1)w. \\
p_3 &= (x-1)^2 + z^2 + w^2 + (x-1)z + (x-1+z)w. \\
p_4 &= (x-1)^2 + (z+1)^2 + w^2 + (x-1)(z+1) + (x-1+z+1)w. \\
p_5 &= x^2 + (z+1)^2 + w^2 + x(z+1) + (x+z+1)w. \\
p_6 &= (x+1)^2 + z^2 + w^2 + (x+1)z + (x+1+z)w.
\end{aligned}$$

Solving these equation will give following equation.

$$\begin{aligned}
p_1 &= p_0 + x - z + 1. \\
p_2 &= p_0 - 2z - x - w + 1. \\
p_3 &= p_0 - 2x - z - w + 1. \\
p_4 &= p_0 - x + z + 1. \\
p_5 &= p_0 + 2z + x + w + 1. \\
p_6 &= p_0 + 2x + z + w + 1.
\end{aligned}$$

Direct layer neighbors of $(x,\ y,\ z,\ w)$ are $U_1(x-1,\ y+1,\ z,\ w+1)$, $U_2(x,\ y+1,\ z-1,\ w+1)$, and $U_3(x,\ y,\ z,\ w+1)$. Distance of them can be written in term of p_0.

$$\begin{aligned}
p_{u1} &= p_0 + w - x + 1. \\
p_{u2} &= p_0 + w - z + 1. \\
p_{u3} &= p_0 + 2w + x + z + 1.
\end{aligned}$$

Our printer nozzle moves from one voxel to its immediate direct neighbor. We do not need to calculate the square of the distance in every voxel. It can be seen from the above equations that instead of calculating the square, we only required addition, subtraction, and multiplication by two (which can be replaced by safe left shift operator). Thus saving a lot of clock cycle in terms of computation.

Theorem 8. Separability in sphere ${D_2}^2 - {D_1}^2 > 2r$ for hollow sphere of radius r

Proof. voxels inside the sphere must satisfy the following equation

$$ {D_1}^2 \leq r^2 - r $$

voxels outside the sphere must satisfy the following equation

$$ {D_2}^2 > r^2 + r $$

$$ {D_2}^2 - {D_1}^2 > 2r $$

□

Theorem 9 (Last voxel in a sphere)**.** For a given value of l, if $p > R2(r_2^2 + r_2)$ at the first voxel for this layer l. Then it is the last voxel of the sphere.

Proof. First voxels at layer l have the coordinates $(-i,\ 2i,\ -i,\ 3i+j)$ where $l = 3i+j$.

Given $[D(-i,\ 2i,\ -i,\ 3i+j)]^2 > R2$
first voxel at immediate upper layer $l+1$ will be $(-i,\ 2i,\ -i,\ 3i+j+1)$ where $l+1 = 3\lfloor (l+1)/3 \rfloor + (l+1)\%3$, $i = \lfloor (l+1)/3 \rfloor$, and $j = (l+1)\%3$.

$$\begin{aligned} [D(-i,\ 2i,\ -i,\ 3i+j)]^2 &> R2. \\ i^2 + i^2 - i^2 + (3i+j)^2 + (-2i)(3i+j) &> R2. \\ 6i^2 + j^2 + 4ij &> R2. \end{aligned} \tag{5.13}$$

For the sake of calculation, we have used $j+1$ as j keeping i constant.

$$\begin{aligned} [D(-i,\ 2i,\ -i,\ 3i+j+1)]^2 &> R2. \\ i^2 + i^2 - i^2 + (3i+j+1)^2 + (-2i)(3i+j+1) &> R2. \\ 6i^2 + j^2 + 4ij + 6i + 1 &> R2. \end{aligned} \tag{5.14}$$

Since i is $\mathbb{Z}^+$ and $6i^2 + j^2 + 4ij > R2$

$$ [D(-i,\ 2i,\ -i,\ 3i+j+1)]^2 > R2. $$

There is no need to check for upper layer voxels. □

Theorem 10 (Last Voxel for the even value of y)**.** For a given even value of y at voxel(x,y,z,w) if $x = z$ and value of $p > R2(r_2^2 + r_2)$, Then it is the last voxel for this value of y.

Proof. Lets consider x=z=a Given $[D(a,y,a,w)]^2 > R2$

$$\begin{aligned} a^2 + a^2 + a^2 + w^2 + 2aw &> R2. \\ 3a^2 + w^2 + 2aw &> R2. \end{aligned}$$

Direct neighbors of this voxel will be $(a+1,y,a-1,w)$ and $(a-1,y,a+1,w)$

$$\begin{aligned}
(D(a+1,y,a-1,w))^2 &= (a+1)^2+(a-1)^2+(a^2-1)+w^2+2aw.\\
(D(a-1,y,a+1,w))^2 &= (a-1)^2+(a+1)^2+(a^2-1)+w^2+2aw.\\
(D(a+1,y,a-1,w))^2 &= 3a^2+w^2+2aw+1>R2.\\
(D(a-1,y,a+1,w))^2 &= 3a^2+w^2+2aw+1>R2.\\
(D(a+1,y,a-1,w))^2 &> R2.\\
(D(a-1,y,a+1,w))^2 &> R2.
\end{aligned}$$

Then no need to check for other voxel for this value of y. □

Theorem 11 (Last Voxel for the odd value of y)**.** For a given odd value of y at voxel(x,y,z,w) if $x=z-1$ and value of $p>R2(r_2^2+r_2)$, Then it is the last voxel for this value of y.

Proof. Lets consider x=z-1=a Given $[D(a,y,a+1,w)]^2>R2$

$$\begin{aligned}
a^2+(a+1)^2+(a+1)a+w^2+(2a+1)w &> R2.\\
3a^2+w^2+2aw+2a+w+2 &> R2.
\end{aligned}$$

Direct neighbors of this voxel will be $(a+1,y,a,w)$ and $(a-1,y,a+2,w)$

$$\begin{aligned}
(D(a+1,y,a,w))^2 &= (a+1)^2+a^2+(a^2+1)+w^2+(2a+1)w.\\
(D(a-1,y,a+2,w))^2 &= (a-1)^2+(a+2)^2+(a-1)(a+2)+w^2+(2a+1)w.\\
(D(a+1,y,a,w))^2 &= 3a^2+w^2+2aw+2a+w+2>R2.\\
(D(a-1,y,a+2,w))^2 &= 3a^2+w^2+2aw+2a+w+2+a+1>R2.\\
(D(a+1,y,a,w))^2 &> R2.\\
(D(a-1,y,a+2,w))^2 &> R2.
\end{aligned}$$

Then no need to check for other voxel for this value of y. □

Algorithm 6 Sphere_print(x_r, y_r, z_r, w_r, r_1, r_2)

$l \leftarrow \left\lceil \sqrt{\frac{r^2}{6}} \right\rceil$
$R1 \leftarrow {r_1}^2 - r_2$, $R2 \leftarrow {r_2}^2 + r_2$
if $R1 == 0$ **then** Plot Voxel (0, 0, 0, 0)
for $i \leftarrow 0$ **to** $l-1$ **do**
    $p0 = 6i^2$, $p = 0$, $vf1$ =false, $vf2$ =false, $hf1$ =false, $hf2$ =false
    for $j \leftarrow 0$ **to** 2 **do**
        $p \leftarrow p0 + j(j+4i)$, $p_{save} \leftarrow p$
        if $p > R2$ **then** break ▷ Theorem 9
        $x \leftarrow 0$, $y \leftarrow 0$, $z \leftarrow 0$, $w \leftarrow 3i+j$ ▷ Move to Voxel(-i,2i,-i,3i+j)
        for $y \leftarrow 0$ **to** $r + \lceil \frac{r_2}{3} \rceil$ **do**
            $hf1$ =false, $hf2$ =false
            if y%2==0 **then**
                $vf1$ =false, $vf2$ =false
                while $|x| \leq r + \lceil \frac{r_2}{3} \rceil$ **do**
                    if $p \leq R2$ & $p > R1$ **then**
                        Plot Voxel $(x-i,\ y+2*i,\ z-i,\ w)$ $vf1$ =true, $hf1$ =true
                    else
                        Move to Voxel $(x-i,\ y+2i,\ z-i,\ w)$
                        if $vf1$ **then** $vf2$ =true
                        $hf2$ =true
                        if $p > R2$ & $x == z$ **then** break ▷ Theorem 10
                        if $vf1$ & $vf2$ & $p > R2$ **then** break
                        $p \leftarrow p - (x-i) + (z-i) + 1$
                        $x \leftarrow x-1$, $z \leftarrow z+1$
                if $p > R2$ & $x == z$ **then** break ▷ Theorem 10
                $p \leftarrow p - 2(z-i) - (x-i) - w + 1$
                $z \leftarrow z-1$, $y \leftarrow y+1$
            else
                $vf1$ =false, $vf2$ =false
                while $|z| \leq r + \lceil \frac{r_2}{3} \rceil$ **do**
                    if $p \leq R2$ & $p > R1$ **then**
                        Plot Voxel $(x-i,\ y+2*i,\ z-i,\ w)$ $vf1$ =true, $hf1$ =true
                    else
                        Move to Voxel $(x-i,\ y+2i,\ z-i,\ w)$
                        if $vf1$ **then** $vf2$ =true
                        $hf2$ =true
                        if $p > R2$ & $x == z-1$ **then** break ▷ Theorem 11
                        if $vf1$ & $vf2$ & $p > R2$ **then** break
                        $p \leftarrow p + (x-i) - (z-i) + 1$
                        $x \leftarrow x+1$, $z \leftarrow z-1$
                if $p > R2$ & $x == z-1$ **then** break ▷ Theorem 11
                $p \leftarrow p - 2(x-i) - (z-i) - w + 1$
                $x \leftarrow x-1$, $y \leftarrow y+1$
            if !$hf1$ & $hf2$ **then** break

Algorithm 7 Sphere_print(x_r, y_r, z_r, w_r, r_1, r_2)

45: $l \leftarrow \left\lceil \sqrt{\frac{r^2}{6}} \right\rceil$
46: $R1 \leftarrow {r_1}^2 - r_2$, $R2 \leftarrow {r_2}^2 + r_2$
47: **for** $i \leftarrow 0$ **to** $l-1$ **do**
48: $p0 = 6i^2$, $p = 0$, $vf1$ =false, $vf2$ =false, $hf1$ =false, $hf2$ =false
49: **for** $j \leftarrow 0$ **to** 2 **do**
50: $p \leftarrow p0 + j(j+4i)$, $p_{save} \leftarrow p$
51: **if** $p > R2$ **then** break ▷ Theorem 9
52: $x \leftarrow 0$, $y \leftarrow 0$, $z \leftarrow 0$, $w \leftarrow 3i+j$ ▷ Move to Voxel(-i,2i,-i,3i+j)
53: **while** $|y| \leq r + \lceil \frac{r_2}{3} \rceil$ **do**
54: $hf1$ =false, $hf2$ =false
55: **if** y%2==0 **then**
56: $vf1$ =false, $vf2$ =false
57: **while** $|x| \leq r + \lceil \frac{r_2}{3} \rceil$ **do**
58: **if** $p \leq R2$ & $p > R1$ **then**
59: Plot Voxel $(x-i,\ y+2*i,\ z-i,\ w)$ $vf1$ =true, $hf1$ =true
60: **else**
61: Move to Voxel $(x-i,\ y+2i,\ z-i,\ w)$
62: **if** $vf1$ **then** $vf2$ =true
63: $hf2$ =true
64: **if** $p > R2$ & $x == z$ **then** break ▷ Theorem 10
65: **if** $vf1$ & $vf2$ & $p > R2$ **then** break
66: $p \leftarrow p + (x-i) - (z-i) + 1$
67: $x \leftarrow x+1$, $z \leftarrow z-1$
68: **if** $p > R2$ & $x == z$ **then** break ▷ Theorem 10
69: $p \leftarrow p + 2(z-i) + (x-i) + w + 1$
70: $z \leftarrow z+1$, $y \leftarrow y-1$
71: **else**
72: $vf1$ =false, $vf2$ =false
73: **while** $|z| \leq r + \lceil \frac{r_2}{3} \rceil$ **do**
74: **if** $p \leq R2$ & $p > R1$ **then**
75: Plot Voxel $(x-i,\ y+2*i,\ z-i,\ w)$ $vf1$ =true, $hf1$ =true
76: **else**
77: Move to Voxel $(x-i,\ y+2i,\ z-i,\ w)$
78: **if** $vf1$ **then** $vf2$ =true
79: $hf2$ =true
80: **if** $p > R2$ & $x == z-1$ **then** break ▷ Theorem 11
81: **if** $vf1$ & $vf2$ & $p > R2$ **then** break
82: $p \leftarrow p - (x-i) + (z-i) + 1$
83: $x \leftarrow x-1$, $z \leftarrow z+1$
84: **if** $p > R2$ & $x == z-1$ **then** break ▷ Theorem 11
85: $p \leftarrow p + 2(x-i) + (z-i) + w + 1$
86: $x \leftarrow x+1$, $y \leftarrow y-1$
87: **if** $!hf1$ & $hf2$ **then** break

5.3 Other Geometric Objects

In this subsection, we will represent other geometric objects namely digital planes and regular tetrahedron on the tetrahedral grid.

Digital Planes

We have introduced our grid as Intersection of four sets of parallel planes. Each set of plane is parallel to the face of the tetrahedron see Figure 5.11. Consider a tetrahedron $ABCD$ whose vertex are $D(0,\ 0,\ 0,\ 0)$, $A(1,\ -1,\ 0,\ 0)$, $B(0,\ -1,\ 1,\ 0)$, $C(0,\ 0,\ 0,\ 1)$. The Vertexes of Tetrahedron are our grid points.

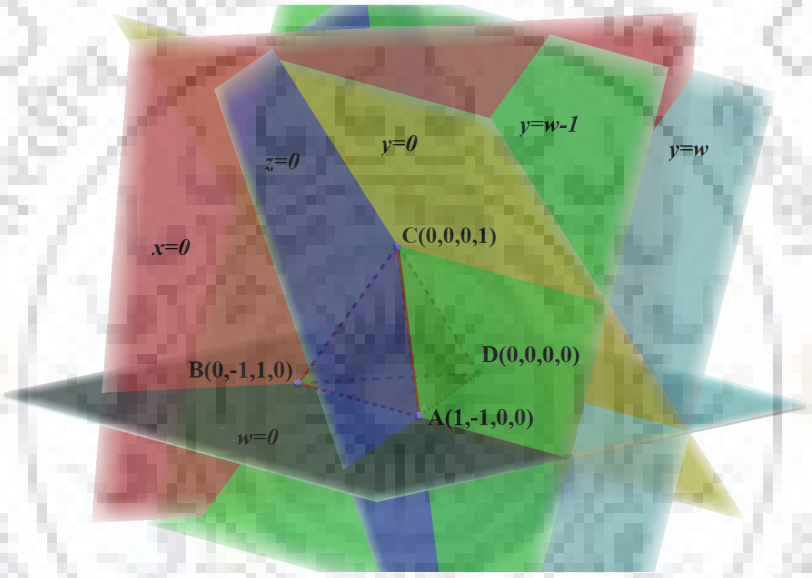

Figure 5.11: Four sets of planes on the tetrahedral grid. $w = 0$ is the plane which is parallel to face ABD represented by black color. $x = 0$ is the plane which is parallel to face BCD represented by red color. $z = 0$ is the plane which is parallel to face ACD represented by blue color. $y = w - 1$ is the plane which is parallel to face ABD represented by green color. $y = w$ is the plane parallel to $y = w - 1$ which passes through point D represented by sky blue color.

Definition 5.2. A tetrahedral grid in 4-coordinate system is infinite intersection of 4 sets of planes. These planes equation is given by $x = t$, $z = t$, $w = t$, $y = w - t$ where $t \in \mathbb{Z}$.

Definition 5.3. A grid point on tetrahedral grid in intersection of

$$x = t_1,\ y = w - t_2,\ z = t_3 \text{ or}$$

$$x = t_1,\ y = w - t_2,\ w = t_4 \text{ or}$$

$$x = t_1,\ z = t_3,\ w = t_4 \text{ or}$$

$$y = w - t_2,\ z = t_3,\ w = t_4.$$

where t_1,t_2, t_3, t_4 are integer.

General plane Equation can be given by $Ax+By+Cz+Dw+E=0$ where A, B, C, D, E are integers. It can not be guaranteed that all point on the plane is valid voxel coordinates. When $A=B=C$, $Dw+E=0$ is a plane parallel to $w=0$ if E is a multiple of D. Recall that $x+y+z=0$ for all voxels.

Definition 5.4. $Ax+By+Cz+Dw+E_1=0$ and $Ax+By+Cz+Dw+E_2=0$ are parallel to each other where A, B, C, D, E_1, E_2 are integers.

Layering a Tetrahedron

Obviously it is easier to represent tetrahedron in our grid because of nature of grid. To layer a tetrahedron we require a point (usually of the base) and side length. In addition to that we require relative position of other two points on the base of tetrahedron in term of sextant. Consider a point in the base of tetrahedron as $V_1(x_1,\ y_1,\ z_1,\ w_1)$. Let the side of tetrahedron as t unit and relative position of other two vertex of the base is sextant-V. Other vertex in the base are $V_2(x_1,\ y_1-t,\ z_1+t,\ w_1)$ and $V_3(x_1+t,\ y_1-t,\ z_1,\ w_1)$. The algorithm to layer a tetrahedron is given as follows.

Algorithm 8 Tetrahedron_layering

```
1: procedure TETRAHEDRON(x_t, y_t, z_t, w_t, t)
2:     x ← x_t   y ← y_t   z ← z_t   w ← w_t
3:     for i = t, i−−, while i ≥ 0 do
4:         for j = 0, j++, while j ≤ i do
5:             x ← x_t   y ← y_t − j   z ← z_t + j   w ← w_t + t − i
6:             for k = 0, k++, while k ≤ j do
7:                 Plot Voxel (x, y, z, w)
8:                 x ← x + 1, z ← z − 1
9: end procedure
```

lemma 1. The number of voxel N_V in a tetrahedron of side t is $\frac{(t+1)(t+2)(t+3)}{6}$.

Proof. From Algorithm 8

$$N_V = \sum_{i=t}^{0} \sum_{j=0}^{i} \sum_{k=0}^{j} 1.$$

$$N_V = \sum_{i=t}^{0} \sum_{j=0}^{i} (j+1).$$

$$N_V = \sum_{i=t}^{0} \frac{(i+1)(i+2)}{2}.$$

$$N_V = \sum_{i=t}^{0} \frac{i^2+3i+2}{2}.$$

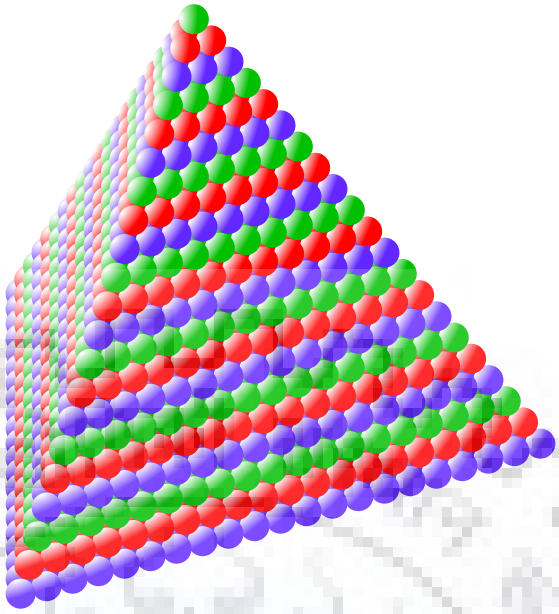

Figure 5.12: Regular Tetrahedron plotted by Algorithm 8 for $t = 20$

$$
\begin{aligned}
N_V &= \frac{1}{2}\left[\sum_{i=0}^{t} i^2 + \sum_{i=0}^{t} 3i + \sum_{i=0}^{t} 2\right].\\
N_V &= \frac{1}{2}\left[\frac{t(t+1)(2t+1)}{6} + \frac{3t(t+1)}{2} + 2(t+1)\right].\\
N_V &= \frac{(t+1)}{2}\left[\frac{t(2t+1)}{6} + \frac{3t}{2} + 2\right].\\
N_V &= \frac{(t+1)}{2}\left[\frac{2t^2+t+9t+12}{6}\right].\\
N_V &= \frac{(t+1)}{2}\left[\frac{t^2+5t+6}{3}\right].\\
N_V &= \frac{(t+1)(t+2)(t+3)}{6}.
\end{aligned}
$$

□

6 Conclusion

We have initially put forward certain approaches to represent geometric objects namely line, circle and arc (or curves) in the 3-coordinates system for the regular simplex grid in 2D. The use of simplex grid has assisted in our transition from 2D to 3D. We have extended three coordinate systems of the simplex grid into a consistent four coordinates system for the tetrahedral grid. We have proposed algorithms for circle, disk, sphere, and tetrahedron. The circle and disk plotting algorithm are efficient. We have given an algorithm for sphere printing for two nozzle printer. These two nozzles can work in parallel.

Sphere packing in tetrahedral grid covers approximately 74% of the volume. Sphere packing in cubic grid covers approximately 52.4% of the volume. If we replace each sphere by rhombic dodecahedron in the tetrahedral grid, then it will tessellation entire space [18].

A natural application of our study on geometric objects on the tetrahedral grid using spherical voxels will be in 3D printing or rapid prototyping [3, 8, 12, 19–21]. Digital 3D printing is evolving. Recently HP Labs and NVIDIA have worked together to overcome the challenges of 3D printing using GVDB voxels [10]. Binding of the individual voxels in 3D printing is a crucial factor for the stability of the printed objects. Due to the self-alignment property of spheres, spherical voxels are proved to be an essential part in 3D printing [6]. Voxels play an important role in 3D printing because voxels can represent complex connected micro structure materials more easily than polygons [5, 7].

Bibliography

[1] B. Das, M. Dutt, A. Biswas, P. Bhowmick, and B. B. Bhattacharya. A combinatorial technique for construction of triangular covers of digital objects. combinatorial image analysis: 16th international workshop. pages 76–90, 2014.

[2] H. Freeman. Algorithm for generating a digital straight line on a triangular grid. *IEEE Transactions on Computers*, C-28(2):150–152, 1979.

[3] H. Glessen, S. Thiele, S. Ristok, and A. Nerkommer. Microstructured optics by 3D printing. In *2017 Conference on Lasers and Electro-Optics Europe European Quantum Electronics Conference (CLEO/Europe-EQEC)*, pages 1–1, June 2017.

[4] I. Her. Geometric transformations on the hexagonal grid. *IEEE Transactions on Image Processing*, 4(9):1213–1222, Sep 1995.

[5] J. Hiller and H. Lipson. Methods of parallel voxel manipulation for 3D digital printing. *18th Annual International Solid Freeform Fabrication Symposium, SFF 2007*, 2007.

[6] J. Hiller and H. Lipson. Design and analysis of digital materials for physical 3D voxel printing. *computer graphics and image processing*, 15(2):137–149, 2008.

[7] J. Hiller and H. Lipson. Design automation for multi-material printing. *20th Annual International Solid Freeform Fabrication Symposium, SFF 2009*, pages 279–287, 2009.

[8] C. L. Huang, C. H. Wen, Y. S. Mao, and J. J. Chen. Applying 3D printing technique to reconstruct cultural artifacts. In *2017 10th International Conference on Ubi-media Computing and Workshops (Ubi-Media)*, pages 1–6, Aug 2017.

[9] R. Klette and A. Rosenfeld. *Digital Geometry*. Morgan Kaufmann, 500 Sansome Street, Suite 400, San Francisco, CA 94111, 2004.

[10] T. Kontzer. How GPUs can kick 3D printing industry into high gear. `https://blogs.nvidia.com/blog/2017/06/06/3d-printing/`. June 6, 2017.

[11] E. Luczak and A. Rosenfeld. Distance on a hexagonal grid. *IEEE transactions of computers*, page 533, 1976.

[12] S. Mafeld, C. Nesbitt, J. McCaslin, A. Bagnall, P. Davey, P. Bose, and R. Williams. Three-dimensional (3D) printed endovascular simulation models: a feasibility study. *Annals of Translational Medicine*, 5(3), 2017.

[13] B. Nagy. Shortest paths in triangular grids with neighbourhood sequences. *Journal of Computing and Information Technology*, CIT 11(2):113, 2003.

[14] B. Nagy. Characterization of digital circles in triangular grid. *Pattern Recognition Letters*, 25(11):1231 – 1242, 2004.

[15] B. Nagy and K. Barczi. *Isoperimetrically Optimal Polygons in the Triangular Grid*. Springer Berlin Heidelberg, Berlin, Heidelberg, 2011.

[16] B. Nagy and R. Strand. Approximating euclidean circles by neighbourhood sequences in a hexagonal grid. *Theoretical Computer Science*, 412(15):1364 – 1377, 2011.

[17] K. Shimizu. Algorithm for generating a digital circle on a triangular grid. *computer graphics and image processing*, 15:401–402, 1981.

[18] R. Strand, B. Nagy, and G. Borgefors. Digital distance functions on three-dimensional grids. *Theoretical Computer Science*, 412(15):1350 – 1363, 2011. Theoretical Computer Science Issues in Image Analysis and Processing.

[19] Y. Sun and Q. Li. The application of 3D printing in mathematics education. In *2017 12th International Conference on Computer Science and Education (ICCSE)*, pages 47–50, Aug 2017.

[20] M. Thiel, Y. Tanguy, N. Lindenmann, F. Niesler, M. Schmitten, and A. Quick. 3D printing of polymer optics. In *2017 Conference on Lasers and Electro-Optics Europe European Quantum Electronics Conference (CLEO/Europe-EQEC)*, pages 1–1, June 2017.

[21] R. K. Vinnakota and D. A. Genov. Self-consistent modeling of laser matter interactions in laser-based 3D printing of metals and alloys. In *2017 Conference on Lasers and Electro-Optics (CLEO)*, pages 1–2, May 2017.